CYCLIC CHANGES OF CYTOPLASMIC COMPONENTS IN RAT SERTOLI CELLS

by

© Adel Antoine Assaf

A thesis submitted to the Faculty of Graduate Studies and Research in partial fulfilment of the requirements for the degree of

Master of Science

Department of Anatomy
McGill University
Montreal, Canada.

August 1980

ABSTRACT

The differential point counting method was used to determine the relative volumes of the various organelles and inclusions in the Sertoli cell cytoplasm at all fourteen stages of the cycle of the seminiferous epithelium in the rat. In a first step, the volume of the Sertoli cell as well as the nuclear-cytoplasmic ratio were estimated, on semithin sections (0.5 μm) stained with toluidine blue, and shown to remain constant from one stage to the other. The data collected on electron microscope photographs revealed that the volumes of certain organelles, such as mitochondria and the saccular component of the Golgi apparatus, did not change significantly during the cycle. However, the density volumes of the tubular component of the Golgi apparatus and of the lysosomes changed appreciably during the cycle, with maximum values at stages II-III and VI-VIII respectively. The relative volume of the subsurface elements of the endoplasmic reticulum (ER) in the Sertoli cell cytoplasm decreased significantly at stages VII to IX. While the distended tubular ER cisternae (mostly smooth) decreased volumetrically at stage IX, the flattened elements of the ER (rough variety) increased markedly at stages VI, VII and VIII. Phagosomes also varied quantitatively reaching a peak at stages VIII and IX. Lastly, the density volume of lipids increased substantially from stages X to XIV of the cycle. Thus, for most of the cytoplasmic components of the Sertoli cell, a marked cyclic variation was observed.

Name: Adel A. Assaf

Title of Thesis: Cyclic changes of cytoplasmic components in rat Sertoli cells.

Department: Anatomy

Degree: Master of Science

RÉSUMÉ

Les volumes relatifs des organites et inclusions du cytoplasme de la cellule de Sertoli, à chacun des quatorze stades du cycle de l'épithélium séminifère du rat, ont été obtenus par la méthode de comptage différentiel de points. En premier lieu, le volume de la cellule de Sertoli ainsi que le rapport noyau-cytoplasme, mesuré sur coupes semifines (0.5 µm) colorées au bleu de toluidine, restent constants au cours du cycle. Les données quantitatives, sur photographies prises au microscope électronique, ont montré que les volumes de certains organites tels que les mitochondries et l'élément sacculaire de l'appareil de Golgi ne changent pas d'une façon significative au cours du cycle. Cependant, la densité de volume de l'élément tubulaire de l'appareil de Golgi et des lysosomes change d'une façon appréciable montrant des valeurs maximales aux stades II-III et VI-VIII respectivement. Le volume relatif des citernes du réticulum endoplasmique (ER) associées à la membrane cytoplasmique de la cellule de Sertoli diminue d'une façon significative aux stades VII, VIII et IX. Tandis que les citernes dilatées et tubulaires du ER (principalement non granuleux) diminuent en volume au stade IX, les éléments aplatis du ER (type granuleux) augmentent d'un façon marquée aux stades VI-VII et VIII. Les phagosomes varient quantitativement atteignant un sommet aux stades VIII et IX. Enfin, le volume des lipides augmente considérablement aux stades X-XIV du cycle. Donc la plupart des composants cytoplasmiques de la cellule de Sertoli varient d'une façon marquée au cours du cycle de l'épithélium séminifère.

Nom: Adel A. Assaf

Titre de la thèse: Evolution des éléments cytoplasmiques des cellules de Sertoli au cours du cycle de l'épithélium séminifère du rat.

Département: Anatomie

Diplôme: Maître ès Sciences

To my beloved Father and Mother

ACKNOWLEDGMENTS

I would like to express my sincere appreciation and gratitude to Dr. Y. Clermont for giving me the privilege of working as a graduate student in the Department of Anatomy under his supervision, and I am deeply indebted to him for his guidance and encouragement, but above all for the patience and understanding he provided throughout this investigation.

I would like to express my thanks to Dr. L.S. Hermo for his expertise in the field of my research. I am also very grateful to Drs. C.E. Smith, N.J. Nadler and J.J.M. Bergeron for helping me in many problems related to stereological and morphometric analysis.

Many thanks to Dr. M.F. Lalli and Ms. Kathryn Hewitt for their excellent technical help in the use of the electron microscope and the techniques associated with it.

My gratitude is also extended to the following members of this Department for the high quality of their work and helpful advice: Mrs. Aliki Dragatakis for photographic printing; Mrs. Margot Oeltzschner for preparing the illustrations and graphs; Mr. Anthony Graham for preparing the photographic reproductions.

I am most grateful to Mrs. Jean Plamondon for her efficiency and dedication in typing the present thesis.

This work was supported through a grant from the Medical Research Council of Canada to Dr. Y. Clermont.

TABLE OF CONTENTS

LIST OF TABLES AND FIGURES

INTRODUCTION

The Sertoli cell, the somatic supporting element of the seminiferous epithelium, has retained the attention of numerous electron microscopists and endocrinologists during the past decade (see reviews by Fawcett, '75; Dym, '77a, b). Its possible role in the maintenance of spermatogenesis, although it is still difficult to define in precise terms, is becoming more evident with time as our understanding of its cellular activities and of its relations with germinal cells is progressing. Certain aspects of the Sertoli cell function have been well documented soon after the discovery of this cell by Sertoli in 1865. For example, the role of the Sertoli cell in the phagocytosis of the residual cytoplasmic bodies which detach from the maturing spermatids has been well described by Regaud at the turn of the century in 1901. More recently with the utilization of sophisticated physiological (micropuncture of seminiferous tubules) and analytical biochemical techniques (Setchel and Waites, '75) as well as the use of freeze fracture preparation techniques and transmission electron microscopy (Dym and Fawcett, '70), a new function of the Sertoli cell has been demonstrated, i.e., its role in the creation of a blood-testis barrier which regulates the passage of certain molecules from a basal to an adluminal compartment in the seminiferous epithelium, thus creating a special milieu in which spermatocytes and spermatids differentiate (see detailed description below). The Sertoli cell is also known to synthesize an androgen binding protein under the stimulation of FSH (Means *et al.*, '76).

However, despite these observations and many others, the cyclic evolution of this non-dividing and apparently stable cell in relation to the cyclical events taking place in the seminiferous epithelium as a whole

has retained the attention of histologists only sporadically (see review by Roosen-Runge ('62) and the present review of the literature). It is the intention of the present thesis to document such cyclical changes taking place in Sertoli cells by performing a stereological analysis of its various organelles, i.e., mitochondria, endoplasmic reticulum, Golgi apparatus and lysosomes at the various stages of the cycle of the seminiferous epithelium. The data collected revealed that while certain cytoplasmic components were not quantitatively modified during the cycle, others underwent significant volumetric or morphometric changes. A correlation between such changes and the activities of the Sertoli cell in relation to events taking place in the seminiferous epithelium will also be discussed.

REVIEW OF THE LITERATURE

Structure of the Sertoli cell at the light microscope

Enrico Sertoli in 1865, working on macerated human seminiferous tubules, succeeded in isolating and distinguishing from germinal cells a large stellate cell that he named a "cellule ramificate." The histologists working on the seminiferous epithelium of other mammals have identified this element and referred to it thereafter as the Sertoli cell, a name still used today. Due to the irregular shape of the Sertoli cell and most of all due to the presence of numerous germinal cells (spermatogonia, spermatocytes and spermatids) in this epithelium, the exact boundaries of such a cell were difficult to demarcate with the light microscope. In fact, several authors (von Ebner, 1871; Regaud, '01; Rolshoven, '45) considered the Sertoli cells as a multinuclear syncytium in which the germinal cells (spermatocytes, spermatids) were embedded. Sertoli himself, however, in

1877 (quoted by Regaud, '01) considered these sustentacular cells as separate cellular entities, a view that was later confirmed by electron microscope investigations (Fawcett and Burgos, '56). Elftman ('50) working with the light microscope noted that the Sertoli cell cytoplasm had a marked capacity for reducing silver, and also considered that these cells were individual cellular units rather than components of a syncytium, an opinion shared by Nishida ('54). Later, Elftman ('63) outlined the cytoplasmic limits with the silver impregnation technique and showed that the basal part of the Sertoli cell cytoplasm was triangular, whereas the apical columnar part could be compared to a tree trunk. The extent of the Sertoli cell cytoplasm from the basement membrane to the lumen of the tubules led Vilar *et al.* ('62) and Mancini *et al.* ('63) to suggest that Sertoli elements act as bridge cells for the transfer of nutrients and metabolites between the intertubular space and tubular lumen. Under the light microscope, the Sertoli cells were readily identified by their large pale stained polymorphous nucleus showing a characteristic centrally located spherical nucleolus (Sertoli, 1865) accompanied by two spherical or cup-shaped bodies of heavily stained chromatin (Bouin, 1899, quoted by Fawcett, '75) now known to be the juxtanuclear bodies or nucleolar associated heterochromatin. Working on the seminiferous tubules of the rat, Regaud ('01) and Leblond and Clermont ('52b) separated the nuclei of Sertoli cells into two types according to their appearance and general orientation in the germinal epithelium: the flat or oval nuclei with their long axis parallel to the limiting membrane, and the triangular or oblong ones which have their long axis perpendicular to the membrane. In a quantitative study of the seminiferous epithelium, Clermont and Perey

('57b) showed that in the rat, the mitotic activity of Sertoli cells ceases completely at 18 days after birth.

Because of the limitations of the light microscope, very few organelles were identified in the Sertoli cell cytoplasm, but the inclusions present were described appropriately. According to Regaud ('09), Benda in 1899 noted the presence of some filamentous structures that he identified as being mitochondria and described them as having different shapes, resembling roundish grains in the basal area and more elongated in the apical part of the Sertoli cell. The same description was given to these elements by Nishida ('54) who, in addition, reported their even distribution throughout the cytoplasm of the Sertoli cell.

In his study on the human seminiferous epithelium, Sertoli (1865) observed pigment granules located between the heads of spermatids. While continuing his investigation on rat Sertoli cells, Regaud ('01) using the high magnification of the light microscope described two sets of secretion vacuoles which were variable in size, shape and content and followed their migration in the epithelium. Leblond and Clermont ('52a) and Roosen-Runge ('55a) were able to stain some of these granules with the periodic acid Schiff technique (PAS). Later, Dietert ('66), Reddy and Svoboda ('67) and Sapsford *et al.* (69b) suggested that these granules were lysosomes and that they might play a role in the resorption of phagocytosed material by the Sertoli cell.

In his description of the Sertoli cell protoplasm, Regaud ('01) observed filamentous or fibrillar material, embedded in an amorphous substance, usually running in the same direction as the long axis of the cell. He suspected that this material could be of contractile nature.

Both Sertoli (1865) and Regaud ('01) reported the presence of large spheres or sometimes small homogeneous spherules mostly at the base of the cell and concluded that they represented lipid droplets. Similar observations were made by Lynch and Scott ('51), Roosen-Runge ('55a), Niemi and Kormano ('65) and Lacy ('62, '67). The latter author believed that the degradation of the lipid droplets in the early stages of the cycle may serve as a means of producing a steroid hormone that might determine the time as well as the synchronization of the meiotic divisions of the germ cells.

Regaud ('01) also observed that small amounts of cytoplasm became separated from the spermatozoa that were being released into the tubular lumen. He was convinced that during normal spermatogenesis, these bulky bodies were phagocytosed by Sertoli cells. Regaud termed these cytoplasmic inclusions "residual bodies" and differentiated them from both degenerating germ cells and phagocytosed spermatozoa. Many years later, several other investigators (Daoust and Clermont, '55; Kingsley-Smith and Lacy, '59; Nicander, '63; Dietert, '66; Sapsford *et al.*, '69b) confirmed the observations of Regaud.

Structure of the Sertoli cell at the electron microscope

With the advent of the electron microscope and appropriate methods of tissue preparations (Porter and Cláude, '45) the interest in the Sertoli cells was revived.

The structure of the Sertoli cell nucleus was reviewed by Bustos-Obregon and Esponda ('74) but very few details were added to what was already known.

One initial contribution that attracted attention was the one of

Fawcett and Burgos ('56) who showed electron photographs of distinct lateral and apical cell boundaries delimited by a continuous membrane of the Sertoli cell. These authors therefore disproved the concept of the syncytial nature of Sertoli cells. Their work helped in the understanding of the Sertoli cell development in the mouse and rat (Sapsford, '63). Working on the bandicoot, Sapsford *et al.* ('67) observed fine cytoplasmic processes extending from the main cell column and divided them into lateral and apical.

Although there have been extensive investigations related exclusively to the germ cells or to the Sertoli cells, the interrelationship between both kinds of cells received little attention at first. Brokelmann ('61) observed peculiar surface layers of the Sertoli cells, which were particularly pronounced around the heads of older spermatids. Later, Brokelmann ('63), Flickinger and Fawcett ('67) and Nicander ('67) noted the presence of junctional specializations between adjacent Sertoli cells. At the site of such a junction, the intercellular space is narrowed to 70-90 Å. There is a layer of cisternae of endoplasmic reticulum parallel to each membrane and 400 Å to 600 Å distant from it. The cisternae bear ribosomes only on the side facing the cytoplasm and the space between these ER elements and the plasma membrane contains periodic densities that appear as a band-like aggregation of fine filaments. The authors also reported analogous junctional specializations between the heads of acrosome phase spermatids (steps 8-19) and Sertoli cells, but in this case there were no ER cisternae nor bundles of filaments within the germ cell cytoplasm. Recently, Romrell and Ross ('79) working on dissociated testicular cells arrived at the same conclusions.

Fawcett et *al*. ('70), Dym and Fawcett ('70) and Dym ('72) demonstrated the existence of a series of linear tight junctions, between adjacent Sertoli cells at the level of a junctional specialization, that formed an effective barrier, i.e., the blood-testis barrier of Setchell and Waites ('75) that prevented penetration of substances of large molecular weight. Ross and Dobler ('75) showed the capacity of these specialized junctional complexes in maintaining firm adhesion between the basal region of adjoining Sertoli cells after efferent ductuli ligation. Dym and Fawcett ('71) and Dym ('73, '77b) in an attempt to clarify the appearance and function of these tight junctions showed that they delimit two compartments within the seminiferous epithelium. The basal compartment which contains the spermatogonia, preleptotene and leptotene spermatocytes and the adluminal compartment which includes the other classes of spermatocytes and spermatids.

Setchell ('67) suggested that Sertoli cells secrete or transport a fluid (water, K^+, myoinositol) from the base of the seminiferous epithelium into the tubular lumen. However, Vitale-Calpe *et al*. ('73) and Fritz and Dorrington ('77) demonstrated that fluid secretion does not start until the formation of the tight junctions between adjcent Sertoli cells. Fritz ('78) showed that both fluid secretion and the formation of the blood-testis barrier are dependent upon stimulation by FSH. Dym ('73, '77b) also noted the presence of various gap junctions located between adjacent Sertoli cells exhibiting a 20 Å interspace. He emphasized that these gap junctions probably permit ions and small molecules to pass from one Sertoli cell to the other. Later, Dym and Cavicchia ('77a, '78) and Russell ('77b) showed that the tight junctions between Sertoli cells break down to allow

the passage of late leptotene or early zygotene spermatocytes, at stage IX of the cycle, from the basal to the adluminal compartment. Fawcett ('74), Gilula *et al.* ('76) and Nagano and Suzuki ('76) working on freeze fracture preparations to examine plasma membranes within seminiferous tubules came to the same conclusions concerning the structural appearance of the intercellular junctions between neighboring Sertoli cells, but showed that there were no membrane specializations to indicate the presence of either tight, gap, desmosome or any other variety of junctions between Sertoli cells and germ cells.

Nevertheless, Kaya and Harrison ('76), Russell (77a) and Gravis ('79), reported the presence of desmosome-like junctions between Sertoli cells and spermatogonia, spermatocytes and young spermatids (steps 1-8) and suggested that these junctions served as strong adhesive sites.

Since von Ebner (1871) first postulated that movements in the Sertoli cell protoplasm may be responsible in the release of the spermatozoa into the tubular lumen (spermiation), several investigators have proposed different mechanisms to explain the role played by the Sertoli cell in this phenomenon. Burgos and Vitale-Calpe ('67, '70) working on the toad and hamster showed that just prior to sperm release, the matrix and cisternae of smooth endoplasmic reticulum in the Sertoli cell apical cytoplasm swell. These authors concluded that this swelling may help in pushing the heads of spermatids into the lumen. This fluid imbibition theory was questionned by Sapsford and Rae ('68), Sapsford *et al.* ('69a), Fawcett and Phillips ('69) and Gravis ('78) who suggested that complex active movements in the apical cytoplasm of Sertoli cells along with the disintegration of the junctional specializations result in the extrusion

of sperm heads while the residual bodies are retained within the germinal epithelium. Lastly, a third explanation was proposed by Ross ('76) who stated that spermiation is initiated through a physiological change that causes a displacement of the junctional specializations between Sertoli cells and the heads of late spermatids and the eventual release of the sperm heads from their attachment sites. He proposed a similar mechanism in relation to the inter-Sertoli junctional complexes to account for the means by which the spermatocytes cross the blood-testis barrier to reach the adluminal compartment of the seminiferous epithelium.

Working on the rat, Russell ('75) and Russell and Clermont ('76) demonstrated that on the ventral concave surface of the sickle-shaped head of a late spermatid (steps 18-19), the plasma membrane develops long narrow tubular projections which invaginate deeply the Sertoli cell cytoplasm. These authors suggested that these so-called tubulobulbar complexes may serve as anchoring devices retaining the spermatids and hence the breakdown of these processes would contribute to sperm release. Later, Russell ('79a, b) showed that the spermatid cytoplasm volume diminished by about 70% between the formation and resorption of these complexes and suggested that the Sertoli cell is a principal agent in the elimination of excess cytoplasm from the spermatid. Russell also showed that the lysosomal population of the Sertoli cell is responsible for the phagocytosis of degenerated tubulobulbar complexes. Finally, Malone ('79) studied these projections in a variety of other species and found some resemblance with those described in the rat.

The structural composition of the Sertoli cell cytoplasm was described in many reviews (Bawa, '63; Brokelmann, '63; Nagano, '66; de Kretser, '68; Schulze, '74; Fawcett, '75; Schulze and Holstein, '76) but

there were very few detailed studies done on the various organelles found in the cytoplasm.

Christensen and Chapman ('59) and Brokelmann ('63) observed the presence of what seemed to be in 3D cup-shaped mitochondria in the Sertoli cell. Brokelmann ('63) also reported the presence of large vesicles of smooth endoplasmic reticulum. Working on human seminiferous tubules, Nagano ('66) demonstrated that the smooth ER is more prominent in the Sertoli cell, whereas the rough ER is poorly developped. Fawcett ('75) localized the granular reticulum mostly in the basal cytoplasm of rat Sertoli cells and described it as being made of tubules and stacks of parallel cisternae, whereas the smooth ER could be first observed around the tip of early acrosome phase spermatids appearing as sharply circumscribed, crescentic or conical masses of membranes in the cytoplasm. Very recently, Clermont *et al.* ('80) separated the endoplasmic reticulum present in the Sertoli cell cytoplasm around the heads of late spermatids (step 19) into two types: Flattened cisternae and tubular cisternae communicating with each other to form a continuous network which, however, undergoes deep structural modifications prior to spermiation.

The Golgi apparatus has been observed in many studies (Nishida, '54; Nagano, '66; Dym, '73; Schulze, '74) as a juxtanuclear organelle and the description given by Fawcett ('75) has generally been accepted. He described it as being formed of multiple separate Golgi complexes, each of which consists of a few short, parallel cisternae and associated small vesicles. In a more extensive study on the Golgi apparatus, Rambourg *et al.* ('79) described its saccular and tubular nature, and by using a special staining technique on thick sections demonstrated that the various Golgi

stacks are communicating with one another via intersaccular connecting tubules.

As was mentioned earlier, many investigators noted the presence of membrane-bound granules in the Sertoli cell cytoplasm (Dietert, '66; Reddy and Svoboda, '67; Sapsford *et al.*, '69b; Fawcett, '75) but very few gave an account of the structure of these granules. Nevertheless, Hermo *et al.* ('78) described these lysosomal elements as being large, often heterogeneous granular-like, or smaller spherical granules with an electron dense core surrounded by a halo. These lysosomes are often arranged in clusters at the base of the cell or in between the heads of late spermatids.

Christensen ('65) was the first to report the presence of microtubules in the Sertoli cell and suggested that they may help in supporting cytoplasmic extensions and produce the movements of spermatids. Later, Dym ('72) observed these elements in the Sertoli cell cytoplasm parallel to the axis of late spermatids and also concluded that they may help in cytoplasmic streaming. Toyama ('76) showed that some of the microfilaments associated with the junctional specializations are actin-like in nature. At the same time, Gravis ('76) localized adenosine triphosphatase in the interface between spermatids and Sertoli cell cytoplasmic processes in association with filaments.

Structural modifications of the Sertoli cell in relation to the cycle of seminiferous epithelium

Sertoli cells and germ cells together make up the seminiferous epithelium which undergoes a cyclic evolution known as the cycle of the seminiferous epithelium (Regaud, '01; Leblond and Clermont, '52b). The

Sertoli cells are the supporting and most stable elements of the epithelium (Dym, '74), intercalated between the various germ cells. The idea that Sertoli cells undergo structural modifications in relation to the cycle of the seminiferous is at least a hundred years old, but the first investigator to carefully analyse this problem was Regaud in 1901. He reported changes in the shape of the Sertoli syncytium and remarkable nuclear deformities and movements from the basement membrane at the twelve stages of the cycle that he identified. He also gave a full account of the contents of the Sertoli cell at each stage of the cycle and concluded from his observations that there are cyclic variations in the amount and distribution of secretion vacuoles, lipid droplets as well as of some fibrillar material found in the cytoplasm at the various stages of the cycle. Rolshoven ('45) also showed changes in the shape of the Sertoli syncytium that can be correlated with the stages of the cycle. Later, Elftman ('50) described cyclical changes in the shape of the individual Sertoli cells. Using their classification of cell associations forming the cycle of the seminiferous epithelium (stages I-XIV) into 14 stages in the rat, Leblond and Clermont ('52b) reported changes in shape and displacement of the Sertoli cell nucleus at specific stages of the cycle. Brokelmann ('61), using the electron microscope, observed surface modifications of the Sertoli cell plasma membrane, more intense at the time of sperm release. Roosen-Runge ('62) suggested that Sertoli cells undergo cyclic behaviour which in turn mediates the proper functioning of spermatogenesis. Russell and Clermont ('76) showed that at the time of sperm release (stages VII-VIII) the Sertoli cell develops large apical drop-like processes, each of which encapsulates and maintains a single sickle-shaped

spermatid head in a juxtaluminal position. These authors showed that this is a periodic event occurring at every cycle of the seminiferous epithelium. And recently, Gravis ('78), using the scanning electron microscope, showed changes in the configuration of the Sertoli cell of the hamster at the different stages of the cycle. All these investigations indicated that during the cycle of the seminiferous epithelium, there is a cyclic modification of the Sertoli cell.

A few studies were undertaken, however, to determine if there are cyclic variations of the cytoplasmic components of the Sertoli cell. Leblond and Clermont ('52a) and Roosen-Runge ('55a) reported variations in the amount and distribution of PAS stainable granules during the cycle of the seminiferous epithelium. Working on the general cytology of Sertoli cells in various mammals, Nishida ('54) observed the presence of numerous granules (lysosomal in nature) in the cytoplasm and noticed that their amount increases when spermatozoa are mature. Later, Sapsford *et al.* ('69b) showed that the number of lysosomes in the bandicoot increases up to the stage of the cycle (VIII) where residual bodies are engulfed by the Sertoli cells. Finally, Hermo and collaborators ('78), studying the distribution of the lysosomes in these cells, concluded that there is an accumulation of these membrane-bound structures at the base of Sertoli cells during stages VI to VIII, whereas from stage IX and onwards most of the lysosomes migrate toward the supranuclear region.

Roosen-Runge ('55a) using radioactive acetate showed a turnover of lipid material in the Sertoli cell associated with certain stages of the cycle in the rat. Lacy ('62) localized the increase in the lipid content of the Sertoli cells during stages X to XIV. Later, Niemi and Kormano ('65)

showed that during stages IX to II, the lipid droplets increased drastically in size and were situated almost entirely at the base forming a narrow sudanophilic ring around the periphery of the seminiferous tubules. Many other investigators reported a lipid cycle in Sertoli cells in other species (Brokelmann, '63; Sapsford *et al.*, 69b; Kerr and de Krester, '75).

Russell ('79c) investigated the formation and resorption of the inter-Sertoli cells tubulobulbar complexes and noticed that these structures arise at stages II to V and are resorbed at stages VI and VII, whereupon their number decreases drastically from stages VII to XIV and I. Russell also reported variations in size and configuration of the tubulobulbar complexes and concluded that these changes occurring at specific stages of the cycle may influence the process of spermatogenesis.

So far no attention has been given to the evolution of other cytoplasmic components of the Sertoli cell, i.e., Golgi apparatus, endoplasmic reticulum and mitochondria, during the cycle.

Histochemical modifications of the Sertoli cell in relation to the cycle of the seminiferous epithelium

There were several cytochemical studies undertaken in the Sertoli cell at the various stages of the cycle in the rat. Niemi and Kormano ('65) showed that there was very little acid phosphatase activity in Sertoli cells from stages IX to XIV and I-II. Later, Reddy and Svoboda ('67) reported an increase in acid phosphatase activity in granules of Sertoli cells at the stages of the cycle just prior to the phagocytosis and breakdown of the residual bodies. By far the most complete study on enzymatic patterns in the Sertoli cell of the rat in relation to the cycle was performed by Hilscher and colleagues ('79). These authors demonstrated that

thiamine pyrophosphatase becomes positive in the basal region of the Sertoli cell from stages XI to XIV. During stages I to IV, the enzyme appears as streams in the body of the cell up to the heads of elongating spermatids. The investigators also showed that adenosine triphosphatase is positive in the apical region of Sertoli cells from stages IX to XI and more concentrated around the heads and middle pieces of elongated spermatids from stages XII to XIV and I to VIII. However, their work on acid phosphatase does not conform with the previous studies by Niemi and Kormano ('65) and Reddy and Svoboda ('67) in that Hilscher *et al.* ('79) experiments showed that acid phosphatase activity was present as diffuse precipitations in the supranuclear region of Sertoli cells during stages XII to XIV and I to III, whereupon it disappeared.

Fabrini *et al.* ('69) working on human testis demonstrated that the glycogen present in the seminiferous tubules is mainly but not exclusively localized in the Sertoli cells and that it plays an important role in the maturation of the germinal cells. These authors also showed that while glycogen is abundant at some stages, it decreases with the first meiotic divisions and is completely absent at other stages of the cycle.

Radioautographic studies done by Kierszenbaum ('74) using ^{3}H-uridine as a precursor showed that there is a rapid turnover of RNA in Sertoli cells during the cycle of the seminiferous epithelium in the mouse.

Working on dissected tubules, Parvinen *et al.* (in press) using the transillumination technique to identify the stages of the cycle, demonstrated that firstly, the maximum ^{125}I-FSH binding on Sertoli cells occurs at stages XIII-XIV and I, is reduced at stages II to VI and is lowest at stages VII and VIII. Secondly, that the highest stimulation of cAMP

production by FSH occurs at stages II-VI and thirdly, that the maximum production of an androgen binding protein is associated with stages VII-VIII, i.e, at the time of sperm release.

All these data suggested a cyclic modification of the functional activity of the Sertoli cells during the cycle of the seminiferous epithelium.

PURPOSE OF THE PRESENT STUDY

The objective of the present investigation was to analyze by a stereological method the potential cyclic evolution of various cytoplasmic structures, i.e., mitochondria, Golgi apparatus, endoplasmic reticulum (of various types), lysosomes, lipid droplets and phagosomes found in the Sertoli cell cytoplasm and to relate these modifications, if they exist, with the cyclic events taking place in the seminiferous epithelium as a whole.

MATERIALS AND METHODS

ANIMAL HANDLING AND PERFUSION TECHNIQUES

Testicular tissue was obtained from four adult Sherman rats aged 3½ to 4 months and weighing approximately 350 to 400 grams. All testes were fixed with 5% glutaraldehyde buffered with 0.2 M s-collidine at pH 7.4 (Bennett and Luft, '59) by a perfusion technique described by Vitale-Calpe *et al.* ('73) which consists briefly of the following steps. After each rat was anaesthetized with nembutal at a dose of 8×10^{-4} ml/gm body weight, an abdominal incision was made exposing the dorsal aorta and left kidney. After clamping the aorta at its point of bifurcation into the common iliac arteries and applying a sutural knot around the same vessel where it divides into renal arteries, lactated Ringer's solution

was introduced in a retrograde direction at the former site, using an 18 gauge needle, as a blood washing procedure. At the same time, the left renal vein was nicked to allow an exit of blood and perfusate. Perfusion with Ringer's solution lasted for 45 seconds after which time the fixative was introduced for a period of 15 to 20 minutes at a relatively constant pressure regulated by gravity.

PROCEDURES FOR ELECTRON MICROSCOPY

Following fixation, thin slices from both right and left testes were cut further into small 1 mm^3 blocks and stored for two hours at $4^{o}C$ in fresh fixative. The tissue was then washed several times at half hour intervals with buffer solution and left over night at $4^{o}C$. Postfixation was carried out on the next day using an aqueous solution of ferrocyanide-reduced osmium tetroxide for two hours at $4^{o}C$. This method was first used by Karnovsky ('71), but was modified in the present experiments to consist of 3% potassium ferrocyanide with 2% osmium tetroxide in a one to one ratio. It has been shown previously in our laboratory that these concentrations enhance the staining of the membranes of organelles and improve their contrast. This technique will be referred to as the Os-K-Ferrocyanide technique. Following postfixation the tissue was dehydrated in graded ethanol solutions ranging from 50% to 100% infiltrated in propylene oxide and finally embedded in Epon (Spurr, '69). After trimming the embedded blocks, semithin sections (0.5 µm thick) were cut on a Reichert Om U2 ultramicrotome, mounted on glass slides and stained with 1% toluidine blue. Following identification of the stages of the cycle (Leblond and Clermont, '52b; Clermont and Perey, '57a), the blocks were further trimmed around selected tubular cross sections and thin sections in the silver

interference colour range (60-90 nm) were cut and mounted on 300 mesh copper grids. The sections were then stained for 5 minutes with uranyl acetate (Watson, '58) and 2 minutes with lead citrate (Reynolds, '63) and finally examined with a Siemens Elmiskop I electron microscope.

IDENTIFICATION OF THE STAGES OF THE CYCLE OF THE SEMINIFEROUS EPITHELIUM

It is now well established that the epithelium lining seminiferous tubules undergoes a cyclic evolution, referred to as the cycle of the seminiferous epithelium and which could be defined as a complete series of successive cellular associations appearing in any given area of a seminiferous tubule (Leblond and Clermont, '52b). As shown by several investigators (see review, Clermont, '72), the cycle can be divided into a constant number of cellular associations or stages depending on the species studied. In the rat, 14 stages have been defined, each containing several generations of cells where a generation is defined as a group of cells at the same step of development. Thus, any particular cellular association includes one generation of spermatogonia, the youngest germ cell line which are sitting directly on the limiting membrane adjacent to the Sertoli cells, one or two generations of spermatocytes generally resting above the spermatogonia, and lastly, one or two generations of spermatids situated closer to the lumen. These distinct generations are never arranged at random but are constantly associated with one another forming cell associations or stages of fixed composition. The duration of each cellular association or stage of the cycle has been determined by Clermont *et al.* ('59) and Clermont and Harvey ('65). In the present study, the criteria used to differentiate the stages of the cycle were similar to those used by Clermont and Rambourg ('78), since in both studies the

semithin sections were stained with toluidine blue. In such sections the developing acrosomic system of spermatids in the course of spermiogenesis is stained deep blue, and the steps of its formation and evolution were used to characterize the various cellular associations occurring in the rat (Figure 1). Other detailed observations, like the structural arrangement of the flagellum extending from spermatids, the relative position of the late spermatids (steps 15-19) in the epithelium, the presence of residual bodies in Sertoli cells and the appearance of the spermatocyte nucleus helped confirm the identification of the stages of the cycle of the seminiferous epithelium in the rat. In the present work stages II and III were grouped together due to their morphological similarities.

SAMPLING PROCEDURES

The sampling procedure began with a random selection of 25 blocks of the testicular tissue from each of the four rats. One semithin section (0.5 µm thick) per block was cut and stained with toluidine blue. The semithin sections were examined under the light microscope to determine the stages of the cycle of the various tubular cross sections present. For each block, two or three transversely cut tubules were selected and the blocks trimmed appropriately. The selection procedure of the tubules ensured that there was a fairly equal sampling of all the stages of the cycle. One single thin section (60-90 nm) per block was cut, stained and examined with the electron microscope. Each thin section provided about 20 micrographs, consequently the total number of micrographs per animal was approximately 500. All the electron microscope photographs of Sertoli cells were taken at a constant magnification of 10,000 and were enlarged by a factor of 3 to yield a final magnification of 30,000.

In order to sample the cytoplasmic components of Sertoli cells and define their relative volumes, micrographs were taken wherever Sertoli cell fields could be found. The areas quantitated were devoid of fixation artifacts and large cytoplasmic vacuoles. Care was taken so that there was no overlapping of fields within the same cell and that no particular cell or part thereof was represented more than once. Nearly 40 photographs of Sertoli cells were taken for each stage of the cycle per animal. The number of pictures needed was determined from the plateau of a cumulative average curve.

In addition to the ultrastructure study of Sertoli cells, a light microscope investigation was carried out at a magnification of 1,000 (under oil) to estimate the volume densities of the Sertoli nucleus and cytoplasm in relation to the Sertoli cell itself. This was done by examining semithin sections (0.5 μm) with the light microscope from the four animals and selecting about 160 tubular cross sections representing all the stages of the cycle of the seminiferous epithelium. About twelve tubular cross sections were examined for every stage of the cycle, but from each, only one area per tubule was chosen at random for the quantitative analysis. Again, the appropriate number of tubules needed per stage was determined from the plateau of a cumulative average curve.

STEREOLOGICAL METHODS

Introduction to stereology

In 1847, the French geologist Delesse proved that the relative volumes of the various components making up a rock can be estimated on random sections by measuring the relative areas of their profiles. In his estimation of volume density, Delesse carefully traced and measured

the area of all profiles contained in a section, added all the areas and divided by the area of the section. The derivation of his principle demonstrated that measurements made on sections can indeed be extrapolated to three-dimensional structures (Weibel and Bolender, '73).

In the last thirty years, the need to quantitate and measure structures, cells and spaces in histological research has arisen, but it was not before the early sixties when Elias and Weibel (quoted by Mathieu and Messier, '73) working on the liver and lung respectively as models, demonstrated that the three-dimensional reconstruction of tissues was possible from histometric measurements. Morphometry, a term originally used by geographers to mean the quantitative description of geographical features, has recently been introduced into the field of microscopic anatomy and ultrastructure (Weibel and Elias, '65). Morphometry can be defined as a method that deals with the measurements of organelles, cells and spaces, whereas stereology is the study concerned with the three-dimensional reconstruction of structures based on measurements obtained from two-dimensional images of light or electron microscopy (Mayhew, '79).

To understand these two approaches, one has to consider some features related to microscopic sections. First, every structure in tissues and cells is usually cut at random; second, an n-dimensional structure of a tissue is represented in the section by an (n-1) dimensional image; bodies are seen as areas, surfaces as lines and lines as points; therefore, we always lose one dimension for the benefit of resolution. Finally, the frequency of profiles representing a certain structure is directly proportional to the actual volume of the structure itself in the tissue sectioned (Weibel *et al.*, '66). There are many different parameters which

can be studied in a tissue such as the number, volume, surface area and length of the linear features of structures. In the present work only volume densities of structures have been measured and, therefore, no other parameters will be studied. The relative volume can be defined as the volume fraction occupied by a particular component, i.e., the Golgi volume contained in the cytoplasmic volume of the Sertoli cell. The terms relative volume, fractional volume and volume density will be used synonymously in the present study. Estimation of relative volumes can be done in several ways: Planimetry which uses a polar or electronic planimeter to trace out the area of all profiles contained in a section, add the areas and divide by the section area; The "cut and weigh" method which briefly consists of using electron micrographs of known weight, cutting all profiles and weighing them. The weight ratio between the profiles and the sheet is a direct estimate of volume density. Presently, both these methods are not used as they are fastidious; the linear integration principle proposed initially in its simplest form by Rosiwal in 1898 (quoted by Weibel and Bolender, '73) consists of projecting a test line of known length and measuring the total length of the line segments included in the profiles. The volume density is then obtained directly from the ratio of profiles area over the section area and finally, the method which is widely used to determine volumetric data is "differential point counting", and as the name implies, it simply consists of counting the number of points of a square lattice contained over the profiles of any structure and relating it to the total number of points on the section (Weibel and Bolender, '73). This method of counting was proposed for the first time by Glagoleff ('33) and has been used since then with certain

modifications. Instead of measuring the areas, as with the planimetric method, and sections, as with the linear, the content of the constituents in the aggregates may be determined by counting the number of points for each constituent. The test points of the lattice can be arranged in any manner (regularly or randomly) but it is required, however, that the pattern of points is independent of the structural arrangement of the tissues and cells to be counted.

Test systems and method of counting

In this study, the relative volumes of Sertoli cell organelles were estimated directly on electron micrographs. The Sertoli cell cytoplasm was identified and delineated using a colored Lumocolor pen, excluding all germ cells, late spermatids deeply inserted in apical recesses of Sertoli cells and nuclei of Sertoli cells. A transparent overlay bearing a regular pattern of 285 points, equally spaced by 13 mm, was then placed over every micrograph in a constant way, and points falling over cytoplasmic profiles were recorded and divided by the total number of points covering the Sertoli cell cytoplasm under surveyance. The geometric center of the point was taken as a means of determining which structure to score in the event of ambiguity, i.e., a point falling over or between two structures (Figure 2). Morphometric measurements of the organelles were obtained using a photomicrograph scale marker.

The relative volumes of the nucleus and cytoplasm of Sertoli cells were determined by examining tubular cross sections from the four animals under the very high (X 1,000) magnification of the light microscope. One area per tubule was selected at random and the volumes determined with an ocular eyepiece grid containing a square lattice of 121 points. By using

a stage micrometer, the lattice was measured to be 85 µm on all sides at the magnification of 1,000, and was moved to cover the whole area selected from the limiting membrane to the lumen of the tubules. Points made by the intersecting lines and falling over Sertoli cell cytoplasm or nuclei were recorded separately. The focus was adjusted constantly using the fine focusing knob in order to have a clearer image of the points hitting Sertoli cells.

CORRECTING FACTORS

Thickness of section

Since the major organelles considered in this quantitative analysis had larger diameters than the thickness of the section, the appropriate correcting factor was disregarded and the value of the Holmes effect (Weibel *et al.*, '66) was not calculated. It was also judged unnecessary to estimate the exact thickness of the sections by the fold technique (Small, '68) and to accept the value given to us by the interference colour of the sections which ranged from 60 to 90 nm.

Compression of the tissue

Compression of the tissue by sectioning causes a reduction of section length by about 10%. This effect is compensated in part by optical distortion of the electron micrographs. Such a correction is again judged irrelevant in point counting volumetry since it can be assumed that all cells and organelles are equally affected (Weibel *et al.*, '69).

Magnification of the electron microscope

The electron microscope was calibrated using a cargon grating replica (Blouin, '77; Blouin *et al.*, '77) and the magnification was calculated to be between 9,200 and 9,400. This value was chosen because it

covered large sampling fields and at the same time permitted the identification of the smallest organelles. The enlarger was also calibrated using a ruler to yield a multiplying factor of three, consequently the final magnification of the electron micrographs was approximately 28,000 ± 400.

RESULTS

PART ONE

STRUCTURE OF THE SERTOLI CELL AS SEEN WITH THE LIGHT MICROSCOPE

At high magnification (X 400, X 1,000) of the light microscope, Sertoli cells were identified readily from the germ cells of the seminiferous epithelium by their larger size. The Sertoli nuclei were located in the basal portion and contained prominent nucleoli (Figure 3). The cytoplasm was columnar in shape and often extended to the lumen. As the cell stained more basophilic with toluidine blue, the plasma membranes of the germ cells were clearly outlined (Figure 3). Furthermore, many spherical granules of different diameters were found in the basal and apical portions of the cell. These granules were recognized as being residual bodies, lipids and lysosomes, and their distribution was stage dependent. For instance, at stage VIII of the cycle, it is possible to identify the large, darkly stained residual bodies present along the lumen of the tubule and many lysosomes found in juxtanuclear positions (Figure 3).

STRUCTURE OF THE SERTOLI CELL AS SEEN WITH THE ELECTRON MICROSCOPE

When viewed with the electron microscope, the Sertoli cell was seen to have a stellate shape, resting on the basal lamina and extending to the lumen (Figure 3'). The cytoplasm was highly irregular, being indented by neighboring germ cells and contained within deep recesses

were the heads of the maturing spermatids (Figure 3'). The nucleus of the Sertoli cell was also large and polymorphous with an indented outline (Figure 3'). The nucleoplasm was homogeneous with scattered small clumps of heterochromatin bound to the surface of the nuclear envelope. A prominent tripartite nucleolar complex occupied the center (Figure 3'). The nucleus was usually located in the basal portion, but during stages V, VI and VII, it was occasionally seen extending into the apical portion of the cell.

The *mitochondria* were very numerous and found throughout the cytoplasm of Sertoli cells (Figures 4, 5, 7). Whereas some were spherical or doughnut-shaped, distributed randomly in the basal portion, others were slender or rod-shaped, oriented parallel to the long axis of the cell in the apical part of the cell (Figures 2, 5). The mitochondria ranged in length from 2 to 5 µm on the average, but on a few occasions reached a length of 12 to 15 µm. Their cristae were either tubular or platelike or a combination of the two, while their matrix appeared homogeneous with the Os-K-ferrocyanide technique. The morphological appearance and distribution of the mitochondria in the cell seemed to be constant at all the stages of the cycle.

The *endoplasmic reticulum* of the Sertoli cell was extensive throughout the cytoplasm and was composed of flattened and distended cisternae. The former were found predominantly in the basal cytoplasm and usually bore ribosomes on their surfaces (Figures 5, 9). Each cisterna was made up of two parallel unit membranes separated by a 30 nm space and measured on the average 3 to 4 µm in length. These flattened components were often closely applied to the surface of mitochondria or around lipid droplets

(Figures 5, 9). Flattened cisternae were also seen adjacent to the Sertoli plasma membrane facing neighboring Sertoli cells or acrosome-phase spermatids (steps 8 to 19). In both areas, the cisternae were parallel to the Sertoli cell membrane and bore ribosomes on the surface facing the cytoplasm, while bundles of fine filaments seen in cross section occupied the layer of cytoplasm between the cisternae and the plasma membrane. These subsurface elements of the endoplasmic reticulum were part of the junctional specializations of the Sertoli cell (Figures 5, 7, 9). Whereas the morphology of the flattened components was constant, the distended elements of the endoplasmic reticulum changed drastically in structure at the different stages of the cycle. During stages I to VI, these cisternae appeared as swollen vesicles or spheroidal elements with an irregular contour and a homogeneously stained content denser than the hyaloplasm (Figure 8). At stages VII and VIII, the distended components became tubular in appearance and often were seen branching and communicating with each other forming an elaborate network oriented in the long axis of the cell (Figure 6). These tubular elements had a smooth contour and bore ribosome occasionally. During the second half of the cycle, the distended elements of the ER appeared as vesicles and spheroidal or oblong elements but which unlike the same elements at early stages were more swollen, larger and showed no regular pattern of organization (Figures 5, 7).

The *Golgi apparatus* was made up of stacks of saccules or dictyosomes interconnected by tubular extensions. Golgi elements were found mainly in juxtanuclear positions, but during stages VII-VIII, they were localized in supranuclear and apical regions (Figures 2, 4, 8). Each saccule was

delimited by two membranes enclosing a thin space, and a stack made up of several of these flattened saccules measured between 125 and 225 nm in thickness. Such a stack was composed of the cis face saccule, 2 to 6 middle saccules and the trans element that was often seen to peel off from the stack (Figure 4). Tubular extensions known as the intersaccular connecting tubules linked Golgi stacks together, and the trans tubular network described by Rambourg *et al.* ('79) was often seen parallel and distant from the stacks (Figure 4). There were no condensing vacuoles or secretory granules close to or in association with the stacks of saccules or the tubular elements of the Golgi apparatus.

The *lysosomal population* in the Sertoli cell consisted of primary and secondary lysosomes. Of the two, the primary lysosomes, also known as dense core granules, were membrane-bound and had a densely stained center surrounded with an electron lucent halo (Figure 7). These granules had a fairly constant internal structure, but their diameter ranged from 100 to 150 nm. On the other hand, the secondary lysosomes were diverse in number, size, shape, content and distribution according to the different stages of the cycle. Such membrane-bound bodies ranged in diameter from 0.3 to 1.0 µm and usually had a spherical or ovoid shape with a smooth or irregular outline and a heterogeneous content (Figures 2, 7, 8). While some contained membranous profiles, others were filled with a granular material; still others were fairly vacuolated. Frequently, small and perfectly spherical lipid droplets were seen within some of these secondary lysosomes. The distribution of the lysosomal population was closely related to the position of the spermatids heads in the apical cytoplasmic recesses of Sertoli cells (Figure 7) except at stages

V, VI and VII where the lysosomes were mainly found in great numbers at the base between the nucleus and the limiting membrane. Many multivesicular bodies and myelin figures were also common amongst the primary and secondary lysosomes.

Degenerating structures, such as residual bodies, phagocytosed germ cells and degenerated organelles were also found in the Sertoli cell cytoplasm. Residual bodies were present at stages VIII and IX where their content usually included lipids, residual mitochondria and a mass of ribonucleoprotein. They were easily identified due to their large size (4 to 8 µm in diameter). At stage VIII of the cycle, the residual bodies were large and mostly found in the apical portion of the cell. During stage IX they were much smaller but more numerous and located evenly between the basal and apical portions of the cell.

The *lipids* in the Sertoli cell cytoplasm were found mainly in the basal area close to the limiting membrane. During stages IX-XIV and I the droplets were large and spherical with diameters of the order of 3 to 6 µm (Figure 9), but in the first half of the cycle they were much smaller and had an irregular contour (Figure 6). Lipid droplets stained homogeneously light to dark grey with the Os-K-Ferrocyanide technique.

Microtubules and filaments were present mainly in the apical portion of the cell where they were seen to run in the direction of the cell axis between the germ cells (Figures 2, 6). Due to the fixation used, they were not always clearly visible.

Collections of microvesicles were also present in the cytoplasm of Sertoli cells. Each collection had a diameter of about 0.4 µm and was composed of many tiny vesicles with a darkly stained contour (Figure 7).

These collections were present at all stages of the cycle.

Other components of the cytoplasm included glycogen particles. cross sections of tubulobulbar complexes (Figure 9) and small vesicles of unknown origin. The *hyaloplasm* also contained many clusters and rosettes of free ribosomes (Figure 5).

PART TWO

After a careful examination of the morphology of Sertoli cells, a stereological analysis was carried out at the light and electron microscope level, the data of which will be presented in the coming section of the results. As mentioned earlier, only volumetric estimates of the various components studied were calculated. For a much clearer understanding and interpretation of the results, the density volumes of the larger and more general components such as the nucleus and cytoplasm will be presented firstly, followed by the respective volumes of the organelles and their subcomponents, if any, in Sertoli cells. All the values in Tables I, II, III and IV are accompanied by their corresponding standard deviations.

QUANTITATIVE LIGHT MICROSCOPY

Study of the variation of the Sertoli cell volume during the cycle of the seminiferous epithelium

In order to determine whether or not the Sertoli cell volume varied or remained constant at the different stages of the cycle, a light microscope investigation was undertaken on semithin sections (0.5 µm) obtained from four animals. The Sertoli cells were identified according to the criteria already mentioned. For the purpose of quantitating, a square lattice of points was inserted in the ocular eyepiece of the light micro-

scope, and those test points falling over Sertoli cells in the area examined were recorded for all the stages of the cycle. The width of the area was always constant, being represented by the 85 μm length of any side of the lattice. However, the distance of the area from base to lumen of the epithelium changed from one stage to the other due to the changes in thickness of the seminiferous epithelium during the cycle. In spite of this fluctuation, the area occupied by Sertoli cells appeared to remain constant for all stages of the cycle. Table I shows the average values of the crude counts of test points falling over Sertoli cells at each stage of the cycle. To determine whether or not the means obtained at the various stages were significantly different from one another, a statistical test was performed in the form of a one-way analysis of variance. The test confirmed that there was no significant variation from one stage to the other. This statistical test will be referred to as the OWAV test. Although the epithelium changed its size, the area occupied by Sertoli cells was relatively constant, hence the relative volume of Sertoli cells was roughly estimated to be 20% to 25% of the seminiferous epithelium. This was done by dividing the number of points falling over Sertoli cells by the total number of points present in the area studied.

Density volumes of the nucleus and cytoplasm in Sertoli cells

The test points falling over Sertoli cells and recorded in Table I were further separated into nuclei and cytoplasmic hits. Again, the crude counts of each component are given in Table I. These values represent the means of all twelve recordings for each stage. After application of the OWAV test, it was evident that both nucleus and cytoplasm occupied constant

volumes of the Sertoli cell at all stages of the cycle. This constancy of the values was further reflected by the small standard deviations associated with the corresponding final averages that take into account all 14 stages of the cycle. It can be seen that at any one stage, the sum of the points falling over the nucleus and cytoplasm was always equal to the number of points associated with the Sertoli cell. Furthermore, examination of the results also revealed that the cytoplasm made up about 90% of the cell volume, leaving the remaining 10% to the nucleus. The errors of all the values in Table I are of the order of 10% to 20%, which suggests that there was no significant variation from one animal to the next.

QUANTITATIVE ELECTRON MICROSCOPY

General partition of the Sertoli cell volume into its components

Following the estimation of the relative volumes of both cytoplasm and nucleus in the Sertoli cell, a systematic and quantitative study was performed on 2,000 micrographs in order to determine the volumetric composition of the various components of the Sertoli cell cytoplasm. The organelles and inclusions were identified according to the morphological description already given. The relative volumes of these components were calculated in percentage and are shown in Table II. The values expressed in that Table (II) took into account all the stages of the cycle. The endoplasmic reticulum included the subsurface, flattened and distended cisternae, as described earlier. Similarly, the Golgi apparatus was represented by both tubular and saccular elements. The primary and secondary lysosomes along with the multivesicular bodies and myelin figures were grouped together under the heading of lysosomes. Cell inclusions took into account the volume of both lipids and degenerated

structures (residual bodies, etc.). Finally, the hyaloplasm made up the remaining volume of the cytoplasm and in addition to the ground substance, it grouped such structures as microtubules, filaments, collection of microvesicles, glycogen particles, small vesicles of unknown origin, free and attached ribosomes and other unidentifiable structures. Table II gives us a general idea of the order of magnitude of the relative volume of each cytoplasmic component in the Sertoli cell cytoplasm.

It was demonstrated earlier that the cytoplasm of Sertoli cells occupied as much as 90% of the cell volume. Using this information, it is simple to convert the relative volumes of the organelles and inclusions in the cytoplasm into relative volumes in the Sertoli cell itself according to the formula given in Table II. The latter shows the converted values, i.e., volumes of the components in the Sertoli cell and, as can be seen, they are lower but proportional to the cytoplasmic ones. They, too, represent the means of all the stages of the cycle. The sum of all the cytoplasmic component volumes makes up 89.8% of the cell volume and the remaining 10.2% corresponds to the nuclear volume. It is evident from both sets of values that the organelle occupying the largest volume is the endoplasmic reticulum (∿13%) followed by the mitochondria (∿10%), whereas the Golgi apparatus makes only 2.4% of the cytoplasm and 2.2% of the Sertoli cell. Furthermore, lysosomes and cell inclusions seem to occupy about the same relative volume of 4.5%. Finally, it can be seen that the standard deviations of the mean values for the cytoplasmic inclusions are too large. This can be explained by the fact that the values greatly varied from one stage to the other, as will be seen later.

TABLE I

Volumetric changes (number of points per tubular area) of Sertoli cells during the cycle of the seminiferous epithelium

Stages of the cycle	I	II-III	IV	V	VI	VII	VIII	IX	X	XI	XII	XIII	XIV	Average
Sertoli cell	30.7±4.9	30.3±5.3	31.1±5.4	30.6±4.0	30.0±2.4	29.9±4.9	30.1±5.0	31.2±3.9	31.9±5.5	31.3±5.3	31.4±5.4	33.0±5.4	32.1±5.3	31.0±0.9
Sertoli Nucleus	3.1±1.0	3.2±0.9	3.1±0.9	3.0±0.9	3.3±0.7	3.2±1.0	3.0±0.9	3.1±1.4	3.2±1.1	3.0±1.2	3.2±1.2	3.4±0.7	3.2±1.0	3.2±0.1
Sertoli Cytoplasm	27.6±4.2	27.1±4.7	28.0±5.1	27.6±3.5	26.7±2.0	26.7±4.8	27.1±4.4	28.1±3.3	28.7±5.1	28.3±4.4	28.2±4.9	29.6±4.8	28.9±5.0	27.8±0.9

TABLE II

Mean relative volumes (%) of cytoplasmic components in Sertoli cells

	Mitochondria	Endoplasmic Reticulum	Golgi Apparatus	Lysosomes	Inclusions	Hyaloplasm
In Sertoli cell (including Nucleus)	9.4 ± 0.6	12.9 ± 1.2	2.2 ± 0.5	4.2 ± 0.6	4.7 ± 2.9	56.2 ± 1.9
In Sertoli cytoplasm	10.5 ± 0.7	14.3 ± 1.3	2.4 ± 0.5	4.6 ± 0.7	5.2 ± 3.2	63.0 ± 2.2

Converting Formula: $\text{Volume of component in cell} = \frac{\text{Volume of component in Cytoplasm} \times 90}{100}$

The volumetric composition of the Sertoli cell cytoplasm into its various components at the different stages of the cycle

The relative volumes in percentages of the cytoplasmic components in the Sertoli cell cytoplasm at the 14 stages of the cycle are expressed in Table III. To avoid confusion, each cytoplasmic component will now be analysed separately, following the order of Table III.

The mitochondrial volume appeared to be fairly constant throughout the cycle. This was further verified using the OWAV test, which showed no significant variation. On the average, the mitochondria made up about 10% of the Sertoli cell cytoplasm.

The relative volume of the total endoplasmic reticulum also appeared fairly constant at all stages of the cycle except for stage IX where it decreased drastically. Application of the OWAV test ($p < .05$) demonstrated that there were statistical variations within the set of values of Table III. The relative volume of the ER was high from stages X-XIV and I-III, decreased slightly at stages IV to VIII and was very low at stage IX, where it made up only 10.9% of the cytoplasm. As was mentioned earlier in the description of the cell, the endoplasmic reticulum was subdivided into subsurface, flattened and distended elements. The relative volumes in percentages of these separate subcomponents of the ER are given in Table IV, and the values from this Table are plotted on a graph (Figure 10) that shows three respective curves. The OWAV test ($p < .05$) was applied for each subcomponent of the reticulum and showed that there were significant variations within every set of values. First, the relative volume of the subsurface component was fairly high from stages XII-XIV and I-VI, then decreased to a very low value at stage VII and remained fairly low from

stages VIII to XI. To localize specifically the significant variations, the Student's t-test ($p < .05$) was applied. This was done by comparing the individual means obtained from each animal at one particular stage, with those obtained at another given stage until all combinations possible were examined. The results of the t-test, shown in Table V, demonstrated that the values obtained for stages I and VII were significantly different from those obtained at the other stages.

Contrary to this, the relative volume of the flattened elements of the endoplasmic reticulum was very high at stages VII and VIII and decreased significantly by more than 60% at stage IX and remained low up to stage XIV (Table IV). The fractional volume then increased slightly up to stage VI. The curve (Figure 10) shows the peak at stages VII and VIII, and the t-test analysis in Table V confirmed these results.

Finally, the values for the relative volume of the distended component of the ER (Table IV) appeared to be proportional to those of the total endoplasmic reticulum (Table III). The results showed that the density volume of the distended elements was high at stages X to XIV and I to III, decreased slightly from stages IV to VII and was very low at stages VIII and IX (Table IV). Application of the Student's t-test ($p < .05$) between all possible combinations revealed that the value at stage IX was significantly lower when compared to stages I-IV, VII, X and XII-XIV, whereas the volume of the distended elements of the reticulum at stages II-III was higher compared to stages IV-VII, VIII and X (Table V). These results are also expressed in graph form (Figure 10).

The relative volume of the Golgi apparatus also underwent a cycle of its own. The Golgi seemed to occupy a higher volume at the early stages

of the cycle (I to IV), then decreased gradually up to stage IX. It increased again at stage X, but then the value dropped at stages XII, XIII and XIV (Table III). Application of the OWAV test ($p < .05$) confirmed that there were variations between the various stages. As for the endoplasmic reticulum, the Golgi apparatus was subdivided into tubular and saccular elements. The relative volumes of both elements at the different stages of the cycle are shown in Table IV. The density volume of the saccular component appeared quite constant, but the OWAV test ($p < .05$) showed variations at the limit of significance within the set of data. Furthermore, the t-test ($p < .05$) localized these variations (Table V) specifically to stages XII and XIV, where the relative volumes were slightly lower. The curve of the density volume of the saccular elements of the Golgi at the different stages of the cycle is also shown (Figure 11). The fractional volume of the tubular elements underwent the same modifications as for the whole Golgi apparatus. This is understandable since the tubular component made up about 75% to 80% of the total Golgi. One can see, furthermore, that the volume of the tubular elements is quite high at stages I to V, decreases gradually up to stage IX, undergoes another peak at X and then decreases to its lowest values at stages XII thru XIV (Figure 11). Therefore, the tubular elements and the whole Golgi apparatus undergo a cycle characteristic of a bimodal curve which simply means the presence of two peaks, one at stages II-III and the other at X. The exact variations between the different stages were localized using the t-test ($p < .05$) and the results are shown in Table V. The main observation that can be made from this Table (V) is that the density volume of the tubular elements of the Golgi apparatus at stages II-III is significantly higher than at all other stages.

The relative volume of the lysosomal population in the cytoplasm of Sertoli cells increased gradually from stages I to VI, achieving a plateau at VI, VII and VIII, and finally decreased significantly at IX whereupon it continued to remain low during the second half of the cycle (Table III). To simplify the analysis, lysosomes were separated and scored as either primary or secondary. Table IV shows the relative volumes of these subcomponents and their curves can also be seen (Figure 12). As shown in both Table and graph, the primary lysosomes occupied an insignificant volume in the cytoplasm, and there were no variations from one stage to the next. This was further confirmed with the OWAV test which denoted no significant changes. In contrast to the primary lysosomes, the volume of the secondary lysosomes underwent marked variations, as suggested by the OWAV test ($p < .05$) and showed a curve that was stage dependent (Figure 12). The volume of these lysosomes increased progressively from stages I to VI whereupon it remained high at stages VI to VIII and then decreased drastically at IX, remaining low up to stage XIII. The value at stage XIV in both Tables III and IV cannot be interpreted, since the standard deviation associated with the mean is about 30% which denoted marked variations amongst the animals for that particular stage. The t-test ($p < .05$) shown in Table V suggests that the volumes of the secondary lysosomes at stages IX and XI are statistically lower relative to stages II to VII. Both Tables IV and V demonstrate that the volume at stage VI is definitely higher compared to stages IX to XIII. This is also clearly seen in graph form (Figure 12).

The remaining volume of the Sertoli cell cytoplasm was divided into degenerating structures, lipids and hyaloplasm (Table III). The density volume of all degenerating structures, grouping together residual bodies

and all degenerated material in the cytoplasm was fairly low (1-2%) at all the stages of the cycle except at stages VIII and IX where it increased drastically reaching a volume of 10.3% of the cytoplasm (Table III). Application of the OWAV test ($p < 0.5$) showed definite variations amongst the values and the Student's t-test ($p < 0.5$) suggested that stage IX was significantly higher than all other stages including VIII. Table III also showed that most of the errors associated with the values were of the order of 30% to 70%. The explanation for these high standard deviations could be that the relative volume of the degenerating structures in the Sertoli cell cytoplasm greatly varied from one animal to the other for any given stage.

As for the lipids, they constituted a small but constant volume of the cytoplasm from stages II up to VIII. Their density volume increased thereafter and remained high for the second half of the cycle (IX-XIV and I). During stage X, the lipids made up as much as 6.4% of the cytoplasm, as shown in Table III. The t-test analysis ($p < 0.5$) revealed that the relative volume of the lipids at any stage from X to XIV was statistically higher compared to stages II to VIII. Again, some of the standard deviations were quite high, suggesting the animals contained different amounts of lipids for the same stage considered.

Finally, the hyaloplasm made up the remaining volume of the cytoplasm which was about 63% on the average, taking into account the 14 stages of the cycle (Table II). When looking at Table III, which shows the relative volume of the hyaloplasm at the different stages of the cycle, one can see slight variations between the values. It is evident that the density volume of the hyaloplasm increases constantly from stages I to V

TABLE III

Relative volumes (%) of organelles in the cytoplasm of Sertoli cells at various stages of the cycle of the seminiferous epithelium

Stages of the cycle	I	II-III	IV	V	VI	VII	VIII	IX	X	XI	XII	XIII	XIV
Mitochondria	11.0±0.8	10.3±1.2	10.0±0.7	10.0±0.9	10.0±0.9	11.5±1.0	11.8±1.2	10.2±2.0	10.0±1.0	9.6±1.0	10.6±0.5	10.6±0.5	11.0±0.9
Endoplasmic Reticulum	15.6±1.3	16.2±1.8	14.4±1.0	13.5±1.4	14.4±1.5	14.2±1.4	13.4±0.6	10.9±1.9	15.1±2.0	14.3±3.3	15.6±2.2	14.6±2.2	14.2±2.5
Golgi Apparatus	2.8±0.3	3.4±0.5	2.9±0.5	2.9±0.7	2.5±0.3	2.5±0.6	2.2±0.7	2.1±0.6	2.8±0.2	2.4±0.3	1.5±0.9	2.1±0.4	1.7±0.3
Lysosomes	4.3±1.0	4.8±0.5	5.2±0.6	4.9±0.6	6.0±0.5	5.1±0.4	5.4±1.1	3.8±0.2	4.3±1.3	3.4±0.7	4.2±1.0	4.0±0.6	4.9±1.5
Degenerating Structures	1.4±0.5	1.2±0.6	1.2±0.7	1.0±0.4	1.8±0.6	1.2±0.8	3.5±2.9	10.3±6.3	1.4±0.7	1.9±1.1	2.3±1.0	1.0±0.6	1.3±0.8
Lipids	3.7±1.5	1.4±0.3	0.6±0.4	0.8±0.8	0.6±0.1	1.9±0.5	1.3±0.6	3.1±1.3	6.4±2.1	4.8±2.0	5.2±2.6	4.0±0.8	4.9±2.0
Hyaloplasm	61.2±2.6	62.7±0.6	65.7±1.6	66.9±1.2	64.7±1.2	63.6±0.7	62.4±2.8	59.6±4.7	60.0±2.0	63.6±1.9	60.6±2.0	63.7±2.6	62.0±1.0

TABLE IV

Relative volumes (%) of the subcomponents of the endoplasmic reticulum, Golgi apparatus and lysosomes in Sertoli cells at the various stages of the cycle of the seminiferous epithelium

Stages of the Cycle		I	II-III	IV	V	VI	VII	VIII	IX	X	XI	XII	XIII	XIV
E.R.	Subsurface	2.3±0.5	1.8±0.7	1.9±0.3	2.0±0.6	1.8±0.7	0.8±0.3	1.4±0.5	1.3±0.4	1.6±0.5	1.6±0.1	2.2±0.5	1.7±0.5	2.1±0.5
	Flattened	1.2±0.5	1.4±0.5	1.0±0.2	1.2±0.3	1.7±0.5	2.2±0.5	2.1±0.8	0.8±0.5	0.8±0.5	0.8±0.2	0.8±0.3	0.7±0.2	0.9±0.4
	Distended	12.1±1.2	13.1±1.4	11.5±1.0	10.3±2.0	11.0±0.9	11.2±1.2	9.9±1.1	8.8±1.5	12.7±1.2	12.0±3.0	12.6±1.5	12.2±1.7	11.2±1.6
Golgi Apparatus	Saccular	0.6±0.1	0.7±0.1	0.7±0.1	0.7±0.3	0.5±0.1	0.6±0.2	0.5±0.2	0.4±0.1	0.6±0.1	0.5±0.1	0.3±0.2	0.5±0.1	0.4±0.1
	Tubular	2.2±0.2	2.7±0.4	2.2±0.4	2.2±0.5	1.9±0.2	1.9±0.5	1.7±0.6	1.6±0.5	2.2±0.3	1.9±0.3	1.2±0.7	1.6±0.3	1.2±0.2
Lysosomes	Primary	0.4±0.2	0.2±0.1	0.2±0.1	0.2±0.1	0.2±0.1	0.2±0.1	0.2±0.1	0.1±0.1	0.4±0.1	0.2±0.1	0.3±0.2	0.3±0.2	0.2±0.1
	Secondary	4.0±0.9	4.6±0.6	5.0±0.6	4.7±0.6	5.8±0.5	4.9±0.4	5.2±1.0	3.7±0.2	4.0±1.2	3.2±0.6	3.9±0.9	3.6±0.6	4.7±1.5

TABLE V

T-test Analysis ($p \leq .05$)

Subsurface E.R.

	I	II-III	IV	V	VI	VII	VIII	IX	X	XI	XII	XIII	XIV
I		+			+	+	+	+	+	+			
II-III	+					+							
IV						+		+					
V						+		+					
VI	+					+							
VII	+	+	+	+	+				+	+	+	+	+
VIII	+												
IX	+		+	+									
X	+					+					+		+
XI	+					+							
XII						+				+			
XIII						+							
XIV						+				+			

Flattened E.R.

	I	II-III	IV	V	VI	VII	VIII	IX	X	XI	XII	XIII	XIV
I					+	+	+						
II-III					+	+		+	+	+	+	+	
IV					+	+	+						
V					+	+						+	
VI	+	+	+	+				+	+	+	+	+	+
VII	+	+	+	+				+	+	+	+	+	+
VIII	+		+					+	+	+	+	+	+
IX		+			+	+	+						
X		+			+	+	+						
XI		+			+	+	+						
XII		+			+	+	+						
XIII		+		+	+	+	+						
XIV					+	+	+						

Distended E.R.

	I	II-III	IV	V	VI	VII	VIII	IX	X	XI	XII	XIII	XIV
I							+	+					
II-III			+	+	+		+	+					
IV		+					+	+					
V		+											
VI		+											
VII								+					
VIII	+	+	+						+				
IX	+	+	+		+			+		+	+	+	+
X							+	+					
XI													
XII								+					
XIII								+					
XIV								+					

Golgi Saccules

	I	II-III	IV	V	VI	VII	VIII	IX	X	XI	XII	XIII	XIV
I											+		+
II-III								+			+		+
IV								+			+		+
V											+		
VI													
VII													
VIII													
IX		+	+										
X											+		
XI													
XII	+	+	+	+					+				
XIII													
XIV	+	+	+										

Golgi Tubules

	I	II-III	IV	V	VI	VII	VIII	IX	X	XI	XII	XIII	XIV
I		+									+		+
II-III	+		+	+	+	+	+	+	+	+	+	+	+
IV		+						+			+		+
V		+						+			+		+
VI		+											+
VII		+											
VIII		+											
IX		+	+	+					+				
X		+						+					+
XI		+											+
XII	+	+	+	+									
XIII		+											
XIV	+	+	+	+	+				+	+			

Secondary Lysosomes

	I	II-III	IV	V	VI	VII	VIII	IX	X	XI	XII	XIII	XIV
I			+	+									
II-III								+	+				
IV	+							+	+			+	
V								+	+				
VI	+							+	+	+	+	+	
VII								+	+			+	
VIII									+				
IX		+	+	+	+								
X					+								
XI		+	+	+	+	+							
XII					+								
XIII			+	+	+								
XIV													

reaching its maximum at stage V, decreases gradually to a minimum in stages IX and X and increases again to stabilize from stages XI to XIV. Following the use of the OWAV test ($p < .05$) which denoted statistical variations inside the set of values, the t-test ($p < 0.5$) was applied and showed that the volume of the hyaloplasm at stage X was significantly lower than those at stages II to VII. The hyaloplasm grouped many structures, as mentioned earlier, some of which were also quantitated, but the data are not shown in Table III. For instance, the relative volume of the few collections of microvesicles found in the Sertoli cell cytoplasm was estimated to be 0.1% at each stage of the cycle. Similarly, the density volume of all vesicles that cannot be associated with any other organelle is of the order of 0.6% of the cytoplasm taking into account all the stages of the cycle. These values, however, are subject to many errors since the size of the components involved is very small.

DISCUSSION

The main objective of our stereological analysis was to estimate the relative volumes of the various organelles in the Sertoli cell cytoplasm at the different stages of the cycle of the seminiferous epithelium. In order to perform such a study, it was first necessary to determine if the overall volume of the cell changed during the cycle. Indeed, if the Sertoli cell volume was changing during the cycle, this would affect the relative volumes of the cytoplasmic components and hence would require a correcting factor for those stages where the Sertoli cell volume was different.

The data collected indicated that for a given segment of the seminiferous tubule, constant in width (85 µm) and including the whole

thickness of the epithelium from the limiting membrane to the lumen, the number of points falling over Sertoli cells was constant at all the stages of the cycle. Since our sample (160 tubular cross sections) was large enough to yield statistically valid means, and that the areas were selected purely at random, we can deduce that in a survey of the whole epithelium, the number of points over Sertoli cells would also be constant from one stage to the other. Moreover, since on the one hand, the number of Sertoli cells per tubular cross section (Clermont and Perey, '57b) or per unit area of a whole mount tubule (Hermo, '72) was constant at all stages of the cycle and on the other hand the number of hits (points) over Sertoli cells in the seminiferous epithelium was also constant, it can be concluded that the average volume of each Sertoli cell does not change appreciably during the cycle (Bolender, '79). Therefore, the figures on the relative volumes of the cytoplasmic components of the Sertoli cell at the different stages of the cycle did not need to be corrected or readjusted.

The fact that this study was done on semithin sections (0.5 μm) examined under the light microscope is the source of some difficulties in the counting method. Toluidine blue outlines well the cytoplasmic limits of Sertoli cells and stains darkly the mitochondria found at the periphery of the germ cells which in turn enhance the contrast of the Sertoli cell cytoplasm. However, the difficulty in identifying the very fine cytoplasmic processes of Sertoli cells between the various germinal elements, due to the limited resolution of the light microscope, results in some error in the estimate of the Sertoli cell volumes. Nevertheless, this error is probably small, since electron microscopy indicates that the fine

cytoplasmic processes of the Sertoli cell constitute only a small fraction of the overall cellular volume. Moreover, the same error is applicable to the counts performed at all stages of the cycle and, therefore, can be ignored for the purpose of our study. Hence it was concluded that the volume of the Sertoli cell (cell body or trunk plus major cytoplasmic processes) relative to the cell itself is constant from one stage to the other.

Roosen-Runge ('55b) showed that in the rat, the absolute volume of the Sertoli cell in μm^3 decreases by about 40% at stage IX of the cycle. This author, however, used very thick sections (8 μm) stained with PAS and acid hemalum in which the cellular limits, even of the main trunk of the cells, were rather difficult to identify. In a more recent study on the monkey, Dym and Cavicchia ('77b) using the electron microscope estimated that the volume of Sertoli cells relative to the seminiferous epithelium increases from 24% at stage I to 32% at stage VII of the cycle. Since we know that a whole generation of mature spermatids (step 19) leaves the epithelium at stage VII, the fraction of the epithelial volume occupied by Sertoli cells will increase, which would account for the high value obtained by Dym and Cavicchia ('77b) at this stage. In the present investigation, the volume of Sertoli cells relative to the seminiferous epithelium was also estimated to vary between 20% and 25% during the cycle. The exact values at all 14 stages of the cycle were not determined since such information was not one of our purposes.

Thus, to summarize, it seems that the actual size (volume) of the Sertoli cell when compared to itself is constant throughout the cycle, as shown by the present study, but the thickness of the seminiferous epithelium

must be changing during the cycle and consequently the volume of the Sertoli cell relative to the size (height) of the epithelium changes correspondingly.

Elftman ('50, '63) and Gravis ('78) reported that the Sertoli cell changes its shape, expanding during the first half of the cycle and retracting thereafter. On the other hand, it is shown by the present work that the volume of the Sertoli cell remains unchanged throughout the cycle. This indicates a possible redistribution of the cytoplasm by active streaming between the base and apex of the cell at the different stages of the cycle.

The results presented also show that the relative volume of both nucleus and cytoplasm in the Sertoli cell remains constant at all stages of the cycle. Leblond and Clermont ('52b) have shown changes in the configuration and shape of the Sertoli cell nucleus between the early and late stages of the cycle, but from the present study it can be stated that the volume of the nucleus is constant during the cycle. The Sertoli cell cytoplasm was very abundant, making up as much as 90% of the cell volume, which is consistent with morphological observations made by Regaud ('01), Elftman ('50) and Nishida ('54).

Many investigators have described a Sertoli cell cycle (Elftman, '50;, '63; Roosen-Runge, '62) and postulated that it is coexistent and co-ordinated with the cycle of the seminiferous epithelium, without studying in detail the structural evolution of the various cell components during the cycle. The only studies related to the cyclical activities of Sertoli cells that are well documented deal with the periodic phagocytosis of residual bodies following sperm release (Regaud, '01; Kingsley-Smith

and Lacy, '59; Nicander, '63; Dietert, '66), the cycle involving the appearance and disappearance of large lipid droplets at the base of these cells (Regaud, '01; Lacy, '62; Niemi and Kormano, '65; Kerr and de Krester, '75) and the movements of the Sertoli cell apical cytoplasm at the time of spermiation (Burgos and Vitale-Calpe, '67, '70; Sapsford and Rae, '68; Sapsford *et al.*, '69a; Fawcett and Phillips, '69; Russell and Clermont, '76). However, these investigations have not provided quantitative data to support their observations.

The present study demonstrates that the relative volume of phagosomes in the Sertoli cell cytoplasm increases dramatically at stages VIII and IX of the cycle. This increase is definitely due to the fact that the Sertoli cell phagocytoses many residual bodies at this particular time during the cycle. Based on morphological and quantitative observations, it appears that these bulky bodies migrate from the tubular lumen to the base of Sertoli cells. We also note a shrinkage of the residual bodies from stage VIII to stage IX, as reported previously by Nicander ('63) who attributed this condensation to a lysis of lipid material and ribonucleoproteins.

During stage IX the relative volume of the phagosomes in the cytoplasm reaches a maximum of 10.3%. Due to this large amount of phagocytosed material, the volume of the cytoplasmic matrix or hyaloplasm decreases to its minimal size (59.5%). At the remaining stages (X-XIV, I-VII) of the cycle, the relative volume of phagosomes in the Sertoli cell cytoplasm seemingly represents debris from phagocytosed germ cells and degenerated organelles (mitochondria, tubulobulbar complexes). This small volume persisting throughout the cycle is consistent with the fact that Sertoli

elements constantly remove dead cells and foreign particles (Clegg and Macmilan, '65; Carr *et al.*, '68).

Our investigation also evaluates quantitatively the amount of lipid material found in Sertoli cells at the different stages of the cycle. The results show that the relative volume of lipids in the Sertoli cell cytoplasm increases at stage IX, i.e., following the phagocytosis of residual bodies. This suggests that lipid droplets may form from the breakdown products of phagocytosed material. Lynch and Scott ('51), Lacy ('62) and Lacy *et al.* ('68) showed that any condition that alters spermatogenesis such as X-irradiation, hypophysectomy, starvation, cryptorchidism and a disturbance in androgen metabolism causes an increase in the number of degenerated germ cells in the seminiferous epithelium followed by a substantial increase in the amount of lipid material in Sertoli cells. Thus it seems that since there is a temporal sequence between the maximum volume of residual bodies and an increase in the volume of lipids at stage IX, followed by the maximum volume of lipid droplets in Sertoli cells at stage X, it is not unlikely that these droplets arise from the dissolution of residual bodies.

Lacy ('62, '67) postulated that the lipids found in Sertoli cells may be a precursor of steroid hormones. Dorrington *et al.* ('76, '78) showed that cultured Sertoli cells from 30 to 40 days old rats synthesize low levels of estradiol and estrone under stimulation by FSH. Assuming that steroid synthesis takes place *in vivo* in Sertoli cells from mature rats, it would still be necessary to demonstrate that the lipid droplets seen in the Sertoli cell cytoplasm serve as precursor material. It is more likely, as proposed by Lynch and Scott ('51) and Kerr and de Krester

('75), and considering their slow disappearance from stages I to VIII that the triglycerides found in lipid droplets are metabolized by the Sertoli cells throughout the cycle of the seminiferous epithelium.

Amongst the various organelles present in the Sertoli cell cytoplasm, small dense core granules were observed and classified as primary lysosomes, since they reacted positively for acid phosphatase localization (M.F. Lalli, unpublished data). Considering, on the one hand, that these primary lysosomes constituted a very small fraction (5%) of the total population of lysosomes, and, on the other hand, that their relative volume in the Sertoli cell cytoplasm was constant at all stages of the cycle, these granules will not be given further attention and our discussion will focus exclusively on the evolution of the secondary lysosomes. The data collected showed that there was a definite cyclic variation in the volume of the Sertoli cell lysosomes during the cycle of the seminiferous epithelium. The changes in volume of the lysosomes probably reflect changes in their number, since lysosomes do not grow beyond a certain size in the Sertoli cell. Sapsford *et al.* ('69b) using the electron microscope noted an increase in the number of lysosoms in Sertoli cells of the bandicoot at the time of sperm release. Their work correlates well with the increase in the volume of lysosomes at stages VI-VIII obtained in the present study on the rat. The changes in volume density of lysosomes in the Sertoli cell cytoplasm could be related to the function of such an organelle as a whole. It has been postulated that lysosomes enable the Sertoli cell to break down phagocytosed residual bodies and dispose of cellular debris in the seminiferous epithelium (Dietert, '66; Reddy and Svoboda, '67; Sapsford *et al.*, '69b). Hugon and

Borgers ('66) observed that after whole body X-irradiation, numerous lysosomal granules in Sertoli cells of the mouse were heavily loaded with acid phosphatase and concluded that these granules play an important part in the resorption of phagocytosed spermatogonia. Recently, Russell ('79a) indicated that the Sertoli cell lysosomes in the rat appeared to be involved in the lysis of degenerating inter-Sertoli cells tubulobulbar complexes and consequently in the decrease in number of these complexes at stage VII of the cycle. The present quantitative analysis is consistent with the view that lysosomes are involved in the breakdown of phagosomes, particularly of the residual bodies. The data show that on the one hand, the lysosomal population increases progressively from stage I to stage VI, achieving a plateau at stages VI-VIII, then decreases rapidly during stage IX of the cycle. On the other hand, the residual bodies appear at the surface of the seminiferous epithelium in late stage VIII of the cycle as the spermatozoa separate from them and are released in the tubular lumen. These residual bodies are then engulfed by the apical cytoplasm of Sertoli cells and while carried down toward the base of the cells during stages VIII and IX they are rapidly lysed and disappear completely from the Sertoli cell cytoplasm by the onset of stage X of the cycle. Thus the decrease in the volume density of lysosomes accompanies the dissolution of residual bodies. It can therefore be speculated that secondary lysosomes merge with the residual bodies (also observed on some electron microscope photographs) and release the hydrolases they still contain, which in turn contribute to the lysis of the content of the phagosomes (residual bodies).

Such a process would consequently result in the rapid and concomittant

disappearance of both the residual bodies and some lysosomes and would explain the significant decrease in the volume of the lysosomes obtained between stages VIII and IX of the cycle.

In the present investigation, the Golgi apparatus was divided into two components, the saccular and the tubular, each of which showed a particular evolution during the cycle of the seminiferous epithelium. The relative volume of the saccular component in the Sertoli cell cytoplasm was fairly constant, and hence these elements seemed to be stable volumetrically from one stage to another. Conversely, the tubular component appeared to be profuse and more abundant at stages II-III. Moreover, the volume density of the tubular elements decreased markedly from stage XII-XIV. Thus it seems that the tubular component of the Golgi apparatus undergoes expansion at the beginning of the cycle (stages I to V) and reduction toward the end of the cycle (stages XII to XIV). The equivalent of this tubular component of the Golgi apparatus in neurons of dorsal root ganglia of mice was shown by Boutry and Novikoff ('75) to react for thiamine pyrophosphatase (TPPase). Other cytochemical studies performed at the light microscope level on adult rat testes by Hilscher *et al.* ('79) demonstrated that from stage I to stage IV of the cycle, TPPase activity seemed to be extending in the Sertoli cell bodies from the basement membrane up to the heads of the elongated spermatids. TPPase then disappeared during stage V of the cycle. Hence, the pattern of TPPase postulated by Hilscher *et al.* ('79) may reflect the increase in the volume of the tubular elements of the Golgi apparatus during the early stages of the cycle (I-V) obtained in the present study.

The fact that the tubular component made up about 75% to 80%

of the whole Golgi apparatus and that it varied volumetrically during the cycle suggests that this component must be important to the functional activity of the Golgi apparatus in Sertoli cells.

It is known that the Golgi apparatus of certain cells such as the neutrophils, is involved in the formation of lysosomes (Flickinger *et al.*, '79). The acid hydrolases contained in the lysosomes, which are actually protein enzymes, would be synthesized in the rough endoplasmic reticulum, transported to the Golgi apparatus, where small lysosomal vesicles would form by budding from the margins of the Golgi elements (Flickinger *et al.*, '79).

The present study indicates that such a relationship possibly exists in the Sertoli cell since the increase in the volume of the tubular component during stages I to V exactly precedes the increase in the number of lysosomes at stages VI-VIII. Thus, based on our quantitative data, one may speculate that the volumetric expansion of the tubular elements of the Golgi apparatus may be related to the formation of new lysosomal granules. The nature of this relation remains to be clarified, however, since secretory granules or dense core granules (primary lysosomes) were not seen at proximity of the Golgi apparatus of these cells (Fawcett, '75; Hermo *et al.*, '78; and the present study).

The endoplasmic reticulum was separated into three subcomponents, each of which will now be analysed.

The relative volume of the subsurface elements in the Sertoli cell cytoplasm decreased periodically at stages VII, VIII and IX of the cycle. This diminution in the volume was significant and substantial and is probably related to the loss of the subsurface elements associated with

step 19 spermatids. Clermont *et al.* ('80) showed that during the long stage VII (63 hrs, Clermont *et al.*, '59; Clermont and Harvey, '65), the flattened cisternae of ER that formed a series of concentric layers located toward the periphery of each Sertoli cell apical process disintegrate. Thus it seems that the decrease in the volume of the subsurface elements at stage VII is due on the one hand to their disintegration inside the Sertoli cell apical processes and, on the other hand, to the fact that these elements were rarely seen along the acrosome of step 7 spermatids. During stages VIII-IX, the volume of the subsurface elements increased slightly but was still low compared to the values obtained for the subsequent stages of the cycle. This can be explained by the fact that the newly formed elements or cisternae in association with steps 8 and 9 spermatids were not yet fully developed since subsurface elements usually extend throughout the entire length of the acrosomic system, parallel to it, which in the case of steps 8 and 9 spermatids does not attain its maximum length. Therefore, the decrease in the volume of the subsurface elements during stages VIII and IX is related to the small size (volume) of these elements.

Russell ('77c) postulated that in the rat Sertoli cells, just prior to sperm release (stage VII), the ectoplasmic specializations (subsurface elements) do not disintegrate but dissociate from step 19 spermatids and migrate down in the Sertoli cell cytoplasm along the plasma membrane and reattach themselves to step 7 spermatids and midpachytene spermatocytes. The author concluded that the subsurface elements are not lost but reutilized and redistributed by the Sertoli cell in a cyclic manner. This process, therefore, implies that the volume of the subsurface

elements is always constant and, formation of new elements is balanced by the resorption of some elements lost during their reutilization. Consequently, Russell's work does not correlate with the morphological observations of Clermont *et al.* ('80) nor with the present quantitative data.

The volume of the flattened elements of the ER that are not associated with the Sertoli cell plasma membrane also underwent marked variations especially during stages VI, VII and VIII, where it increased significantly. It was shown that these elements were studded with ribosomes on all their surfaces and consequently making this particular type of ER the site of protein synthesis (Fawcett, '67; Palade, '75). The Sertoli cell, like most mammalian cells, secretes protein in the form of androgen binding protein (Louis and Fritz, '77; Tung and Fritz, '77) and seven major polypeptides with molecular weights ranging from 16,000 to 140,000D (Wilson and Griswold, '79). But very few studies determined if protein synthesis in Sertoli cells occurs on a constant basis or at certain periods during the cycle of the seminiferous epithelium. Nevertheless, Irons ('80) showed that one hour after injection of tritiated proline into the testis of mature rats, the Sertoli cell bodies were heavily labeled at stages VI and VII of the cycle. Irons ('80) concluded that proline must be incorporated into newly synthesized proteins in the Sertoli cell cytoplasm at these specific stages. Furthermore, Parvinen *et al.* (in press) reported that maximal production of androgen binding protein occurs at stages VII and VIII of the cycle. The results of the above investigators indicate that protein synthesis in rat Sertoli cells seems to be activated or initiated during stages VI-VII and VIII of the cycle. However, it is also possible that there is more protein synthesized by Sertoli cells during

stages VI-VII. This latter view may well explain the increase in the volume of the flattened elements of the granular reticulum obtained at the same stages of the cycle (VI-VIII).

The relative volume of the distended elements of the ER in the Sertoli cell cytoplasm was fairly constant except at stage IX when it decreased markedly. These quantitative data reflect the morphology of this particular type of ER. It was observed that during stage IX, the tubular network of ER present at stages VII and VIII collapsed and seemingly dispersed into small and irregular vesicular cisternae. This is certainly the cause of the decrease in the volume of the distended elements of the ER at stage IX of the cycle. During the subsequent stages, i.e., X to XIV, the vesicles and cisternae of ER swelled and definitely contributed to the increase in volume of the ER. The exact function of this type of endoplasmic reticulum in the Sertoli cell and the significance of its volumetric changes during the cycle remain to be clarified.

CONCLUSION

The volume of the Sertoli cell estimated on semithin sections (0.5 µm) was shown to remain constant throughout the cycle of the seminiferous epithelium. Therefore, no corrections needed to be made on the relative volumes of the individual cytoplasmic components of the Sertoli cell. The volume densities of the nucleus and cytoplasm were also unchanged during the cycle. The differential point counting method performed on 2,000 electron micrographs revealed that while some organelles in the Sertoli cell cytoplasm do not change volumetrically, others do undergo significant variations at the different stages of the cycle. The relative volumes of the mitochondria, primary lysosomes and saccular elements of the Golgi

apparatus in the Sertoli cell cytoplasm remained constant throughout the cycle. However, the tubular component, which made up 75% of the Golgi apparatus, increased markedly in volume during the early stages of the cycle (I-V) preceding the increase in the volume and number of the secondary lysosomes at stages VI to VIII. Many of the lysosomes appeared to be used in the breakdown of the phagocytosed residual bodies, and this probably contributed to their decrease in volume during stage IX of the cycle. The dissolution of the residual bodies coincided with the appearance of large lipid droplets that persisted throughout the end of the cycle (stages X-XIV). The endoplasmic reticulum was subdivided into three types according to morphological criteria. The flattened elements of the ER associated with the plasma membrane or subsurface elements decreased volumetrically at the mid stages of the cycle (VII-IX) due to the disintegration of elements associated with step 19 spermatids. Conversely, the flattened elements of the ER with attached ribosomes on all their surfaces, increased in volume at stages VI, VII and VIII and this was taken as an indication that more protein was being synthesized by Sertoli cells. Finally, the relative volume of the distended vesicles and cisternae of the ER (mostly smooth) decreased significantly at stage IX of the cycle of the seminiferous epithelium.

Thus it seems that not only the shape of the Sertoli cell is modified during the cycle but also most of the cytoplasmic components of this cell show a cyclic evolution.

LITERATURE CITED

Bawa, S.R. 1963 Fine structure of the Sertoli cell of the human testis. J. Ulstrast. Res. 9: 459-474.

Bennett, H.S., J.H. Luft 1959 S-collidine as a basis for buffering fixatives. J. Biophys. Biochem. Cytol. 6: 113-114.

Blouin, A., R.P. Bolender, E.R. Weibel 1977 Distribution of organelles and membranes between hepatocytes and nonhepatocytes in the rat liver parenchyma. J. Cell Biol. 72: 441-455.

Blouin A. 1977 Morphometry of liver sinusoidal cells. In: Kupffer cells and other liver sinusoidal cells. Proc. of the Inter. Kupffer Cell Symp., North Holland Biomedical Press, Amsterdam, pp. 61-71.

Bolender, R.P. 1979 Surface area Ratios. I. A stereological method for estimating average cell changes in membrane surface areas. Anat. Rec. 194: 511-522.

Boutry, J.M., A.B. Novikoff 1975 Cytochemical studies on Golgi apparatus, GERL and lysosomes in neurons of dorsal root ganglia in mice. Proc. Nat. Acad. Sci. 72: 508-512.

Brokelmann, J. 1961 Surface modifications of Sertoli cells at various stages of spermatogenesis in rat. Anat. Rec. 139: 211 (Abstract).

_____ 1963 Fine structure of germ cells and Sertoli cells during the cycle of the seminiferous epithelium in the rat. Z. Zellforsch. Mikroskop. Anat. 59: 820-850.

Burgos, M.H., R. Vitale-Calpe 1967 The mechanism of spermiation in the toad. Am. J. Anat. 120: 227-252.

_____ 1970 (see Vitale-Calpe, R., M.H. Burgos).

Bustos-Obregon, E., P. Esponda 1974 Ultrastructure of the nucleus of human Sertoli cells in normal and pathological testis. Cell Tis. Res. 152: 467-475.

Carr, I., E.J. Clegg, G.A. Meek 1968 Sertoli cells as phagocytes: An electron microscopic study. J. Anat. 102: 501-509.

Christensen, A.K., G.B. Chapman 1959 Cup-shaped mitochondria in interstitial cells of the albino rat testis. Exptl. Cell Res. 18: 576-579.

Christensen, A.K. 1965 Microtubules in Sertoli cells of the guinea pig testis. Anat. Rec. 151: 335 (Abstract).

Clegg, E.J., E.W. Macmilan 1965 The uptake of vital dyes and particulate matter by the Sertoli cells of the rat testis. J. Anat. 99: 219-229.

Clermont, Y., B. Perey 1957a The stages of the cycle of the seminiferous epithelium of the rat: Practical definitions in PA-Schiff-hematoxylin and hematoxylin-eosin stained sections. Rev. Can. Biol. 16: 451-462.

_____ 1957b Quantitative study of the cell population of the seminiferous tubules in immature rats. Am. J. Anat. 100: 241-267.

Clermont, Y., C.P. Leblond, B. Messier 1959 Durée du cycle de l'épithélium séminal du rat. Arch. d'Anat. Micros. Morph. Exp. 49: 37-56.

Clermont, Y., S.C. Harvey 1965 Duration of the cycle of the seminiferous epithelium of normal, hypophysectomized and hypophysectomized-hormone treated albino rats. Endocrinology 76: 80-89.

Clermont, Y. 1972 Kinetics of spermatogenesis in mammals: seminiferous epithelium cycle and spermatogonial renewal. Phys. Rev. 52: 198-235.

Clermont, Y., A. Rambourg 1978 Evolution of the endoplasmic reticulum during rat spermiogenesis. Am. J. Anat. 151: 191-212.

Clermont, Y., J. McCoshen, L. Hermo 1980 Evolution of the endoplasmic reticulum in the Sertoli cell cytoplasm encapsulating the heads of late spermatids in the rat. Anat. Rec. 196: 83-99.

Daoust, R., Y. Clermont 1955 Distribution of nucleic acids in germ cells during the cycle of the seminiferous epithelium in the rat. Am. J. Anat. 96: 255-283.

De Krester, D.M. 1968 Ultrastructural studies on the human Sertoli cell. J. Anat. 103: 215 (Abstract).

Dietert, S.E. 1966 Fine structure of the formation and fate of the residual bodies of mouse spermatozoa with evidence for the participation of lysosomes. J. Morph. 120: 317-346.

Dorrington, J.D., I.B. Fritz, D.T. Amrstrong 1976 Testicular estrogens: Synthesis by isolated Sertoli cells and regulation by FSH. In: Regulatory mechanisms of male reproductive physiology. Ed. by C.H. Spilman et al., Experta Medica, Amsterdam, pp. 63-70.

_____ 1978 Control of testicular estrogen synthesis. Biol. Reprod. 18: 55-64.

Dym, M., D.W. Fawcett 1970 The blood-testis barrier in the rat and the physiological compartmentation of the seminiferous epithelium. Biol. Reprod. 3: 308-326.

_____ 1971 Further observations in the numbers of spermatogonia, spermatocytes and spermatids connected by intercellular bridges in the mammalian testis. Biol. Reprod. 4: 195-215.

Dym, M. 1972 The fine structure of the monkey Sertoli cell and its role in establishing the blood-testis barrier. Biol. Reprod. 7: 129 (Abstract).

_____ 1973 The fine structure of the monkey (Macaca) Sertoli cell and its role in maintaining the blood-testis barrier. Anat. Rec. 175: 639-656.

_____ 1974 The fine structure of the monkey Sertoli cells in the transitional zone at the junction of the seminiferous tubules with the tubuli recti. Am. J. Anat. 140: 1-26.

_____ 1977a The role of the Sertoli cell in spermatogenesis. In: Male reproductive system. Ed. by R. Yates, M. Gordon, Raven Press, New York. pp. 155-169.

_____ 1977b The male reproductive system. In: Histology. Ed. by L. Weiss, R. Greep. McGraw Hill, New York, pp. 979-1039.

Dym, M., J.C. Cavicchia 1977a Further observations on the blood-testis barrier in monkeys. Biol. Reprod. 17: 390-403.

_____ 1977b Relative volume of Sertoli cells in monkey seminiferous epithelium: A stereological analysis. Amer. J. Anat. 150: 501-507.

_____ 1978 Functional morphology of the testis. Biol. Reprod. 18: 1-15.

Ebner, V.V. 1871 Untersuchungen uber den Bau der samencanalchen und die Entwicklung der Spermatozoiden bei den Saugethieren und beim Menschen. Leipzig: Untersuchungen aus dem Institute fur Physiologie und Histologie im Graz. 2: 200-236.

Elftman, H. 1950 Sertoli cell cycle in the mouse. Anat. Rec. 106: 381-393.

_____ 1963 Sertoli cells and testis structure. Am. J. Anat. 113: 25-32.

Fabbrini, A., M. Re, C. Conti 1969 Glycogen in the normal human testis: A histochemical and histoenzymatic study. J. Endocr. 43: 499-506.

Fawcett, D.W., M.H. Burgos 1956 The fine structure of the Sertoli cells in human testis. Anat. Rec. 124: 401 (Abstract).

Fawcett, D.W. 1967 The Cell: Its organelles and inclusions. Ed. by W.B. Saunders, Philadelphia and London.

Fawcett, D.W., D.M. Phillips 1969 Observations on the release of spermatozoa and on changes in the head during passage through the epididymis. J. Reprod. Fert. Suppl. 6: 405-418.

Fawcett, D.W., L.V. Leak, P.N. Heidger 1970 Electron microscopic observations on the structural components of the blood-testis barrier. J. Reprod. Fert. Suppl. 10: 105-122.

Fawcett, D.W. 1974 Interactions between Sertoli cells and germ cells. In: Serono symposium on male fertility and sterility. pp. 13-35.

_____ 1975 Ultrastructure and function of the Sertoli cell. In: Handbook of Physiology. Sec. 7, Endocrinology, Vol. 5. Male reproductive system. Ed. by D.W. Hamilton and R.O. Greep, Amer. Phys. Soc., Washington. pp. 21-55.

Flickinger, C.J., D.W. Fawcett 1967 Junctional specializations of the Sertoli cells in the seminiferous epithelium. Anat. Rec. 158: 207-222.

Flickinger, C.J., J.C. Brown, H.C. Kutchai, J.W. Ogilvie 1979 Medical Cell Biology. Ed. by W.B. Saunders, Philadelphia, London and Toronto.

Fritz, I.B., J.D. Dorrington 1977 Summary of the Proceedings of the 4th Testis Workshop. Mol. Cel. End. 9: 121-132.

Fritz, I.B. 1978 Sites of action of androgens and FSH on cells of the seminiferous tubule. Bio. Act. Horm. 5: 249-281.

Gilula, N.D., D.W. Fawcett, A. Aoki 1976 The Sertoli cell occluding junctions and gap junctions in mature and developing mammalian testis. Devel. Biol. 50: 142-168.

Glagoleff, A.A. 1933 On the geometrical methods of quantitative mineralogic analysis of rocks. In: Inst. Econ. Min. Metal. Moskau, pp. 1-55.

Gravis, C. 1976 Light and electron microscopic localization of ATPase in normal and degenerating testes of Syrian hamsters. Am. J. Ant. 147: 419-432.

_____ 1978 A scanning electron microscope study of the Sertoli cell and spermiation in the Syrian hamster. Am. J. Anat. 151: 21-38.

_____ 1979 Interrelationships between Sertoli cells and germ cells in the Syrian hamster. Z. Mikroskop. Forsch. 93: 321-342.

Hermo, L. 1972 Quantitative study of the spermatogonial stem cell population of the rat. Master of Science Thesis, McGill University, Montreal, Canada.

Hermo, L., Y. Clermont, M. Lalli, A. Rambourg 1978 Distribution of lysosomes in Sertoli cells during the cycle of the seminiferous epithelium of the rat. In: 9th Int. Cong. on Elect. Microscop. Ed. by J.M. Sturgess, Imperial Press, Ontario. p. 690 (Abstract).

Hilscher, B., D. Passia, W. Hilscher 1979 Kinetics of the enzymatic pattern in the testis. I. Stage dependence of enzymatic activity and its relation to cellular interactions in the testis of the Wistar rat. Andrologia 11: 169-181.

Hugon, J., M. Borgers 1966 Ultrastructural and cytochemical changes in spermatogonia and Sertoli cells of whole-body irradiated mice. Anat. Rec. 155: 15-31.

Irons, M. 1980 The formation of the flagellum in the rat spermatid. Ph.D. Thesis, McGill University, Montreal, Canada.

Karnovsky, M.J. 1971 Use of ferrocyanide-reduced osmium tetroxide in electron microscopy. Proc. of 11th Am. Soc. Cell Biol., New Orleans. p. 284 (Abstract).

Kaya, M., R. Harrison 1976 The ultrastructure relationships between Sertoli cells and spermatogenic cells. J. Anat. 121: 279-290.

Kerr, J.B., D.M. de Krester 1975 Cyclic variations in Sertoli cell lipid content throughout the spermatogenic cycle in the rat. J. Reprod. Fert. 43: 1-8.

Kierszenbaum, A. 1974 RNA synthetic activities of Sertoli cells in the mouse testis. Biol. Reprod. 11: 365-376.

Kingsley-Smith, B.V., D. Lacy 1959 Residual bodies of seminiferous tubules of the rat. Nature 184: 249-251.

Lacy, D. 1962 Certain aspects of testis structure and function. Brit. Med. Bull. 18: 205-208.

_____ 1967 The seminiferous tubules in mammals. Endeavour 26: 101-109.

Lacy, D., G.P. Vinson, P. Collins, J. Bell, P. Fryson, J. Pudney, A.J. Pettitt 1968 The Sertoli cell and spermatogenesis in mammals. Proc. of 3rd Int. Cong. End. pp. 1019-1029.

Leblond, C.P., Y. Clermont 1952a Spermiogenesis of rat, mouse, hamster and guinea pig as revealed by the "periodic acid-fuchsin sulfurous acid technique." Amer. J. Anat. 90: 167-216.

_____ 1952b Definition of the stages of the cycle of the seminiferous epithelium in the rat. Ann.N.Y. Acad. Sci. 55: 548-573.

Louis, B.G., I.B. Fritz 1977 Stimulation by androgens of the production of androgen binding protein by cultured Sertoli cells. Mol. Cel. End. 7: 9-16.

Lynch, K.M., W.W. Scott 1951 Lipid distribution in Sertoli cell and Leydig cell of rat testis as related to experimental alterations of the pituitary-gonad system. Endocrinology 49: 8-14.

Malone, J. 1979 A study of Sertoli-spermatid tubulobulbar complexes in selected mammals. Anat. Rec. 143: 610 (Abstract).

Mancini, R.E., J.L. LaTorre, M.I. Perez Del Carro, O. Vilar 1963 Histophysiological aspects of the Sertoli cell. Anat. Rec. 145: 336 (Abstract).

Mathieu, O., P.E. Messier 1973 Principes et méthodes de la stéréologie tels qu'appliqués au domaine de l'ultrastructure cellulaire. Rev. Can. Biol. 32: 31-63.

Mayhew, T.M. 1979 Basic stereological relationships for quantitative microscopical anatomy - a simple systematic approach. J. Anat. 129: 95-105.

Means, A.R., J.L. Fakunding, C. Huckins, D.J. Tindall, R. Vitale 1976 Follicle stimulating hormone, the Sertoli cell and spermatogenesis. In: Recent progress in hormone research. Vol. 32. Ed. R.O. Greep, Academic Press, New York. pp. 477-527.

Mori, H., A.K. Christensen 1980 Morphometric analysis of Leydig cells in the normal rat testis. J. Cell Biol. 84: 340-354.

Nagano, T. 1966 Some observations of the Sertoli cell in the human testis. Z. Zellforsch. Mikroskop. Anat. 83: 375-397.

Nagano, T., F. Suzuki 1976 Freeze fracture observations on the inter-cellular junctions of Sertoli cells and Leydig cells in the human testis. Cell Tiss. Res. 166: 37-48.

Nicander, L. 1963 Some ultrastructural features of mammalian Sertoli cells. J. Ultrastruc. Res. 8: 190 (Abstract).

_____ 1967 An electron microscopical study of cell contacts in the seminiferous tubules of some mammals. Z. Zellforsch. Mikroskop. Anat. 83: 375-397.

Niemi, M., M. Kormano 1965 Cyclical changes in and significance of lipids and acid phosphatase activity in the seminiferous tubules of the rat testis. Anat. Rec. 151: 159-170.

Nishida, T. 1954 Cytoplasmic cytology of the Sertoli cells of mammals. Cytologia 19: 203-216.

Palade, G.E. 1975 Intracellular aspects of the process of protein synthesis. Science. 189: 347-358.

Parvinen, M., V. Hansson, E.M. Ritzen (In Press) Functional cycle of Sertoli cells.

Porter, K.R., A. Claude 1945 A study of tissue culture cells by electron microscopy. J. Exp. Med. 81: 232-255.

Rambourg, A., Y. Clermont, L. Hermo 1979 Three-dimensional architecture of the Golgi apparatus in Sertoli cells of the rat. Am. J. Anat. 154: 455-475.

Reddy, K.J., D.J. Svoboda 1967 Lysosomal activity in Sertoli cells of normal and degenerating germinal epithelial cells of rat testis. Am. J. Pathol. 51: 1-18.

Regaud, C. 1901 Etudes sur la structure des tubes séminifères et sur la spermatogénèse chez les mammifères. Arch. d'Anat. Microscop. 4: 101-156, 231-380.

_____ 1909 Etudes sur la structure des tubes séminifères et sur la spermatogénèse chez les mammifères. Arch. d'Anat. Microscop. 11: 291-431.

Reynolds, E.S. 1963 The use of lead citrate at high pH as an electron opaque stain in electron microscopy. J. Cell Biol. 17: 208-212.

Rolshoven, E. 1945 Spermatogenese und Sertoli-syncytium. Z. Zellforsch. Mikroskop. Anat. 33: 439-460.

Romrell, L.J., M.H. Ross 1979 Characterization of Sertoli cell germ cell junctional specializations in dissociated testicular cells. Ann. N.Y. Acad. Sciences 55: 548-573.

Roosen-Runge, E.C. 1955a Cytological and cytochemical changes of the Sertoli cell throughout the spermatogenetic cycle of the rat. Anat. Rec. 121: 358 (Abstract).

_____ 1955b Quantitative studies on spermatogenesis in the albino rat. Ant. Rec. 123: 385-398.

_____ 1962 The process of spermatogenesis in mammals. Biol. Rev. 37: 343-377.

Ross, M., J. Dobler 1975 The Sertoli cell junctional specializations and their relationship to the germinal epithelium as observed after efferent ductuli ligation. Anat. Rec. 183: 267-291.

Ross, M. 1976 The Sertoli cell junctional specializations during spermiogenesis and at spermiation. Anat. Rec. 186: 79-104.

Russell, L.D. 1975 A new type of spermatid - Sertoli cell and Sertoli Sertoli cell connection in the rat testis. Anat. Rec. 181: 469 (Abstract).

Russell, L.D., Y. Clermont 1976 Anchoring device between Sertoli cells and late spermatids in rat seminiferous tubules. Anat. Rec. 185: 259-277.

Russell, L.D. 1977a Desmosome-like junctions between Sertoli and germ cells in the rat testis. Am. J. Anat. 148: 301-313.

_____ 1977b Movement of spermatocytes from the basal to the adluminal compartment of the rat testis. Am. J. Anat. 148: 314-328.

_____ 1977c Observations on rat Sertoli ectoplasmic specializations in spermatogenesis of the rat. Tissue and Cell. 9: 475-498.

_____ 1979a Further observations on tubulobulbar complexes formed by late spermatids and Sertoli cells in the rat testis. Anat. Rec. 194: 213-232.

_____ 1979b Spermatid-Sertoli tubulobulbar complexes as devices for elimination of cytoplasm from the head region of late spermatids of the rat. Anat. Rec. 194: 233-246.

_____ 1979c Observations on the inter-relationships of Sertoli cells at the level of the blood-testis barrier: Evidence for formation and resorption of Sertoli-Sertoli tubulobulbar complexes during the spermatogenic cycle of the rat. Am. J. Anat. 155: 259-279.

Sapsford, C.S. 1963 The development of the Sertoli cell of the rat and mouse: Its existence as a mononucleate unit. J. Anat. 97: 225-238.

Sapsford, C.S., C.A. Rae, K.W. Cleland 1967 Ultrastructural studies on spermatids and Sertoli cells during early spermiogenesis in the bandicoot Perameles nasuta Geoffroy (Marsupalia). Austr. J. Zool. 15: 881-909.

Sapsford, C.S., C.A. Rae 1968 Sertoli cell-spermatid relationships ultrastructural studies of the movements of mature spermatids into the lumen of the seminiferous tubule. J. Anat. 103: 214-215.

Sapsford, C.S., C.A. Rae, K.W. Cleland 1969a Ultrastructural studies on maturing spermatids and on Sertoli cells in the bandicoot (Perameles nasuta). Austr. J. Zool. 17: 195-292.

Sapsford, C.S., C.A. Rae, K.W. Cleland 1969b The fate of residual bodies and degenerating germ cells and the lipid cycle in Sertoli cells in the bandicoot Perameles nasuta Geoffroy (Marsupalia). Austr. J. Zool. 17: 729-753.

Schulze, C. 1974 On the morphology of the human Sertoli cell. Cell Tiss. Res. 153: 338-355.

Schulze, C., A.F. Holstein 1976 On the morphology of the human Sertoli cells under normal conditions and in patients with impaired fertility. Andrologia 8: 167-178.

Sertoli, E. 1865 Dell'esistenza di particolari cellule ramificate nei canalicoli seminiferi del testicolo umano. Il Morgagni. 7: 31-41.

Setchell, B.P. 1967 Fluid secretion by the testes. J. Reprod. Fert. 14: 347-348.

Setchell, B.P., G.M. Waites 1975 The blood-testis barrier. In: Handbook of Physiology. Sec. 7 Endocrinology, Vol. 5. Male Reproductive System. Ed. by D.W. Hamilton and R.O. Greep, Amer. Phys. Soc., Washington. pp. 143-172.

Small, J.V. 1968 Measurement of section thickness. Proc. of the 4th Europ. Conf. for Elec. Micros. pp. 609-610.

Spurr, A.R. 1969 A low viscosity epoxy resin embedding medium for electron microscopy. J. Ultrastruc. Res. 26: 31-43.

Toyama, Y. 1976 Actin-like filaments in the Sertoli junctional specializations in the swine and mouse testis. Anat. Rec. 186: 477-492.

Tung, P.S., I.B. Fritz 1977 Isolation and culture of testicular cells: A morphological characterization. In: Techniques of human andrology. Ed. by E.S. Hafez, North Holland Biomedical Press, Amsterdam, pp. 125-143.

Vilar, O., M.I. Perez Del Cerro, R.F. Manami 1962 The Sertoli cell as a "bridge cell" between the basal membrane and the germ cells. Exptl. Cell Res. 27: 158-161.

Vitale-Calpe, R., M.H. Burgos 1970 The mechanism of spermiation in the hamster. J. Ultrastruct. Res. 31: 381-394.

Vitale-Calpe, R., D.W. Fawcett, M. Dym 1973 The normal development of the blood-testis barrier and the effects of clomiphene and estrogen treatment. Anat. Rec. 176: 333-344.

Watson, M.L. 1958 Staining of tissue sections for electron microscopy with heavy metals. J. Biophys. Biochem. Cytol. 4: 475-478.

Weibel, E.R., H. Elias 1965 Quantitative methods in morphology In: Proc. of the Symp. in Quant. Methods in Morph. during the 8th Int. Cong. of Anat. Ed. by E.R. Weibel, H. Elias, Springer-Verlag, Wesbaden.

Weibel, E.R., G.S. Kistler, W.F. Scherle 1966 Practical stereological methods for morphometric cytology. J. Cell Biol. 30: 23-38.

Weibel, E.R., W. Staubli, H.R. Gnagi, F.A. Hess 1969 Correlated morphometric and biochemical studies on the liver cell. I. Morphometric model, stereologic methods and normal morphometric data for rat liver. J. Cell Biol. 42: 69-91.

Weibel, E.R., R.P. Bolender 1973 Stereological techniques for electron microscopic morphometry. In: Principles and techniques of electron microscopy. Vol. 3. Ed. by M.A. Hayat, Van Nostrand Reinhold Company, New York, pp. 238-296.

Wilson, R., M. Griswold 1979 Secreted proteins from rat Sertoli cells. Exptl. Cell Res. 123: 127-135.

ABBREVIATIONS

(for Figures 2-9)

BL	- Basal lamina
CM	- Collection of microvesicles
DC	- Distended core granule or primary lysosome
dER	- Distended elements of the endoplasmic reticulum (ER)
fER	- Flattened elements of the ER
subER	- Subsurface elements of the ER
Gs	- Saccules of the Golgi apparatus
Gt	- Tubules of the Golgi apparatus
IT	- Interstitial tissue
js	- Junctional specialization
L	- Secondary lysosome
Lip	- Lipid droplet
M	- Mitochondria
Mt	- Microtubules
N	- Nucleus of Sertoli cell
n	- Nucleolus of Sertoli cell
P	- Primary spermatocyte
PM	- Plasma membrane
R	- Ribosomes
RB	- Residual body
SE	- Seminiferous epithelium
SP	- Spermatid
TBC	- Tubulobulbar complex
TL	- Tubular lumen

Figure 1

The 14 cellular associations or stages observed in the seminiferous epithelium of the rat. Each vertical column, depicted by a Roman numeral, represents a cellular association and shows the various cell types present at that stage. The stages of the cycle are identified by means of 14 of the 19 steps of spermiogenesis (numbers 1 to 19). These steps are defined by the changes observed in the nucleus and acrosomic system in semithin sections (0.5 µm thick) stained with toluidine blue.

The cellular associations or stages of the cycle succeed one another in time in any given area of the seminiferous epithelium according to the sequence indicated from left to right in the figure. Following stage XIV, stage I reappears so that the sequence starts over again. The succession of the 14 stages makes up the cycle of the seminiferous epithelium. The duration of each stage in hours is also given. The mitotic divisions of the spermatogonia are indicated by the letter M.

The germ cells present are:

A_1, A_2, A_3, A_4	-	Type A spermatogonia
In	-	Intermediate-type spermatogonia
B	-	Type B spermatogonia
Pl	-	Preleptotene primary spermatocytes
L	-	Leptotene primary spermatocytes
Z	-	Zygotene primary spermatocytes
P	-	Pachytene primary spermatocytes
Di	-	Diplotene primary spermatocytes
II	-	Secondary spermatocytes
1 to 19	-	Steps of spermiogenesis

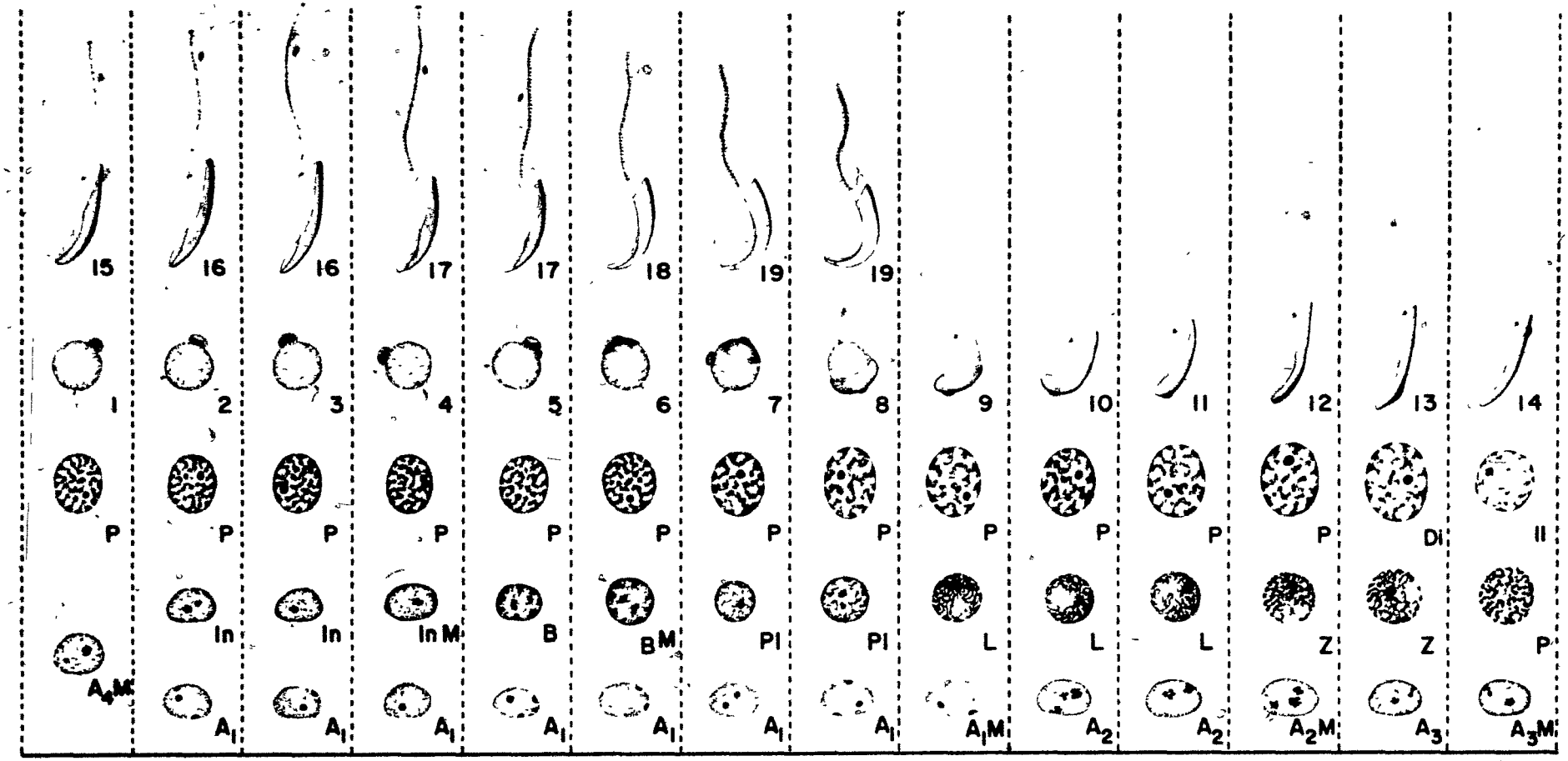
15 16 16 17 17 18 19 19
1 2 3 4 5 6 7 8 9 10 11 12 13 14
P P P P P P P P P P P P Di II
In In In M B B M PI PI L L L Z Z P
A4M A1 A1 A1 A1 A1 A1 A1 A1M A2 A2 A2M A3 A3M
I II III IV V VI VII VIII IX X XI XII XIII XIV
OURS 40 17 10 12 29 27 58 30 7 7 7 31 18 15

①

FIGURE 2

An electron photograph showing the apical region of the Sertoli cell cytoplasm at stage II of the cycle.

(X 36,000)

The black points that are superimposed on the picture and interspaced by 13 mm (½") belong to the test system of points used to estimate the relative volumes of the various cytoplasmic components.

The cytoplasm of the Sertoli cell was delimited using a colored pen, i.e., outline its boundaries thus eliminating the portion of spermatids (SP) that are seen at the upper and lower right-hand corners.

We then recorded the number of points falling over every structure in the Sertoli cell cytoplasm, such as Golgi elements (Gs, Gt), mitochondria (M) and lysosomes (L). The center of the point was used as a means of determining precisely the exact profile that the point overlay. We also recorded the number of points falling over the whole area of the cytoplasm. (See Materials and Methods for further explanation.)


L
Gs
L
Gt
Mt
SP
2

FIGURE 3

Light micrograph showing a portion of a seminiferous tubule at stage VIII of the cycle. (X1,000)

The seminiferous epithelium (SE) is surrounded by a limiting membrane and interstitial tissue (IT). The mature spermatozoa are expulsed into the tubular lumen (TL) leaving behind their residual cytoplasm. The Sertoli cells are depicted by the arrows. Even at this low magnification, we can recognize the nucleus, nucleolus and bulk of cytoplasm filled with granulations.

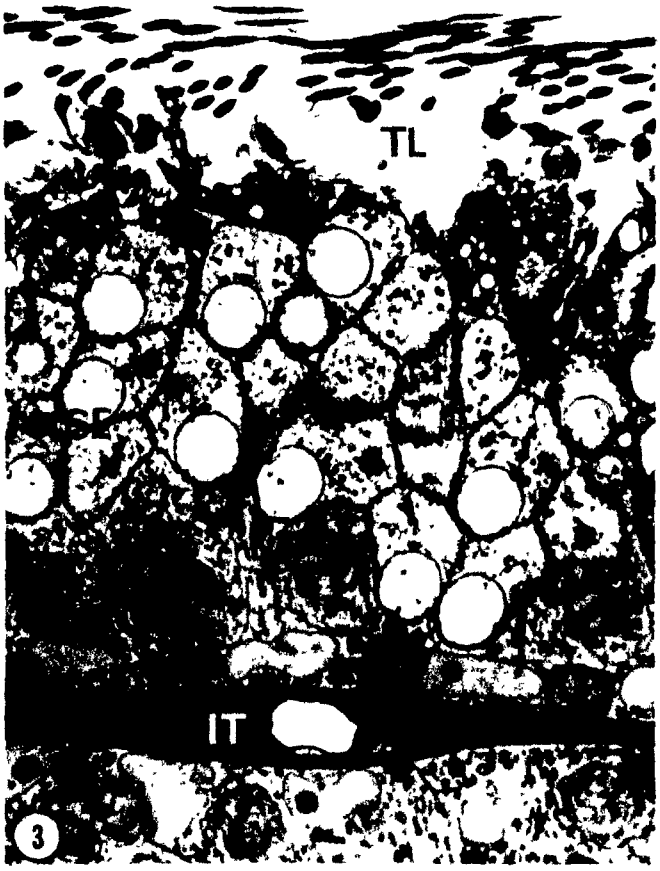
TL
IT
3

FIGURE 3'

The Sertoli cell at two different stages of the cycle. The cell extends from the basal lamina (BL) to the lumen of the tubule. The Sertoli cell nucleus (N) is large and contains a tripartite nucleolus (n). During stage V of the cycle, the elongated heads of rat spermatids (17) are deeply inserted in the Sertoli cell cytoplasm. Whereas, at stage VIII, these spermatids (19) are now located at the surface of the seminiferous epithelium. The Sertoli cell maintains the spermatids in this juxtaluminal position by means of large apical drop-like processes, each of which encapsulates a single sickle-shaped spermatid's head. The Sertoli cell also phagocytoses the residual bodies (RB) at this stage.

This schematic drawing also shows the various junctional specializations (js) of the Sertoli cell.

Also labeled: A_1 - Type A_1 spermatogonium

P - Pachytene spermatocytes

Pl - Preleptotene spermatocyte

5, 8 - Steps of spermiogenesis

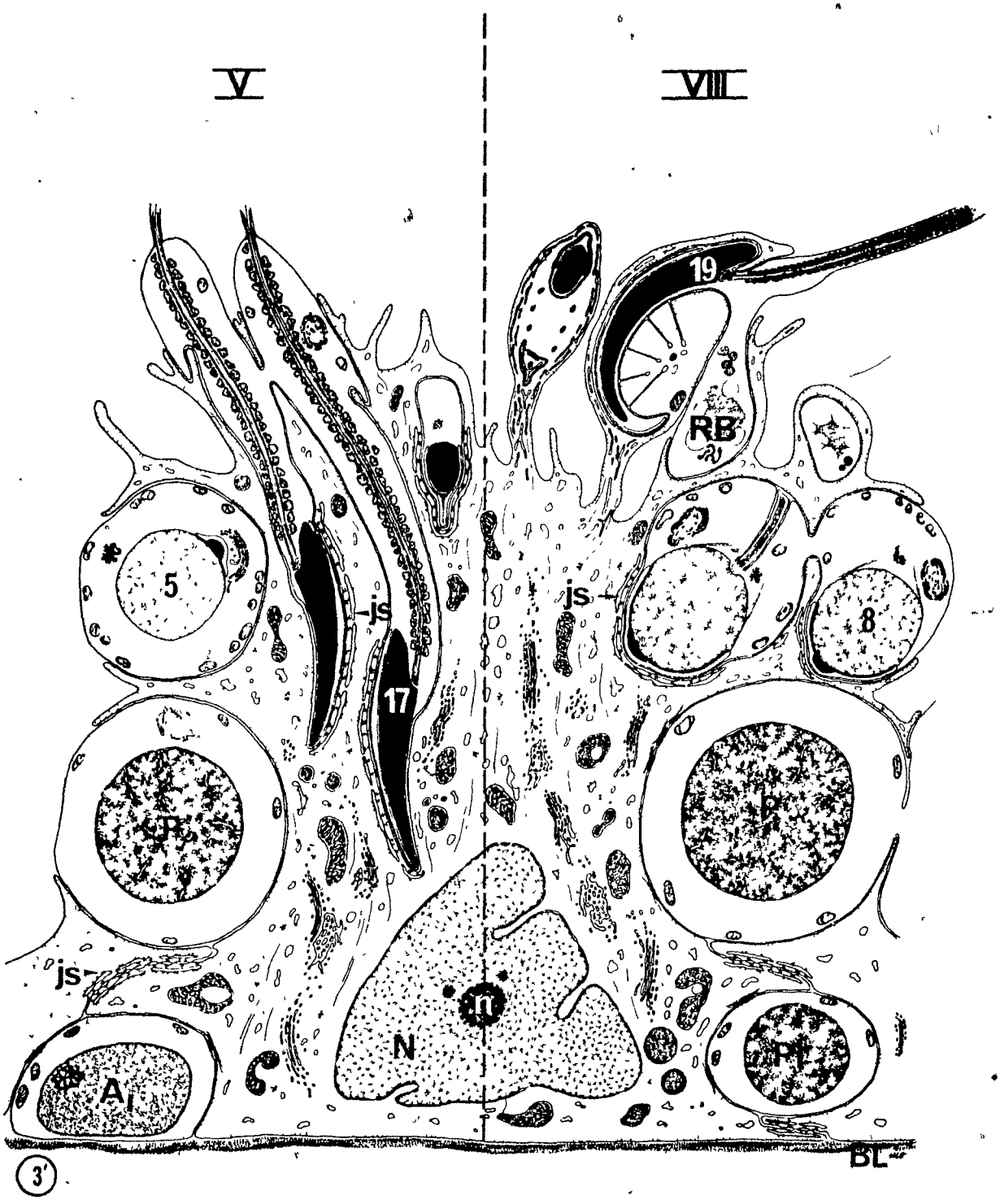
V
VIII
19
RB
5
js
17
8
P
P
js
js
N
A
PL
BL
3'

FIGURE 4

The cytoplasm of the Sertoli cell at the base of the seminiferous epithelium at stage X of the cycle.

(X 30,000)

The basal lamina (BL) and a portion of a primary spermatocyte (P) are seen.

The plasma membranes (PM) of two adjacent Sertoli cells come together at the site of a junctional specialization.

The Golgi apparatus is separated into Golgi saccules (Gs) and Golgi tubules (Gt). The trans saccule and trans tubular network are also seen. The mitochondria (M) have different shapes, often found in proximity to flattened elements of the endoplasmic reticulum (fER). The distended cisternae of the ER (dER) are present throughout the cytoplasm.


dER
P
Gs
fER
PM
Gt
4
BL

FIGURE 5

The basal cytoplasm of the Sertoli cell at stage XI of the cycle. (X 36,000)

This photograph shows clearly the three types of ER that were identified: The flattened elements associated with the plasma membrane (subER); the flattened elements that are not associated with the plasma membrane (fER), and the distended cisternae of the endoplasmic reticulum (dER).

Also shown, clusters of ribosomes (R), doughnut-shaped profile of a mitochondrion (M) and the plasma membranes (PM) of two Sertoli cells.

FIGURE 6

The apical region of the Sertoli cell cytoplasm squeezed in between two spermatids (SP) at stage VII of the cycle. (X 30,000)

The distended elements of the ER (dER) are now tubular-like in appearance, often seen branching and interconnected to form a continuous network oriented in the long axis of the cell.

Microtubules (Mt) are also seen running parallel to the network of endoplasmic reticulum. A small and irregular lipid droplet is present (Lip).

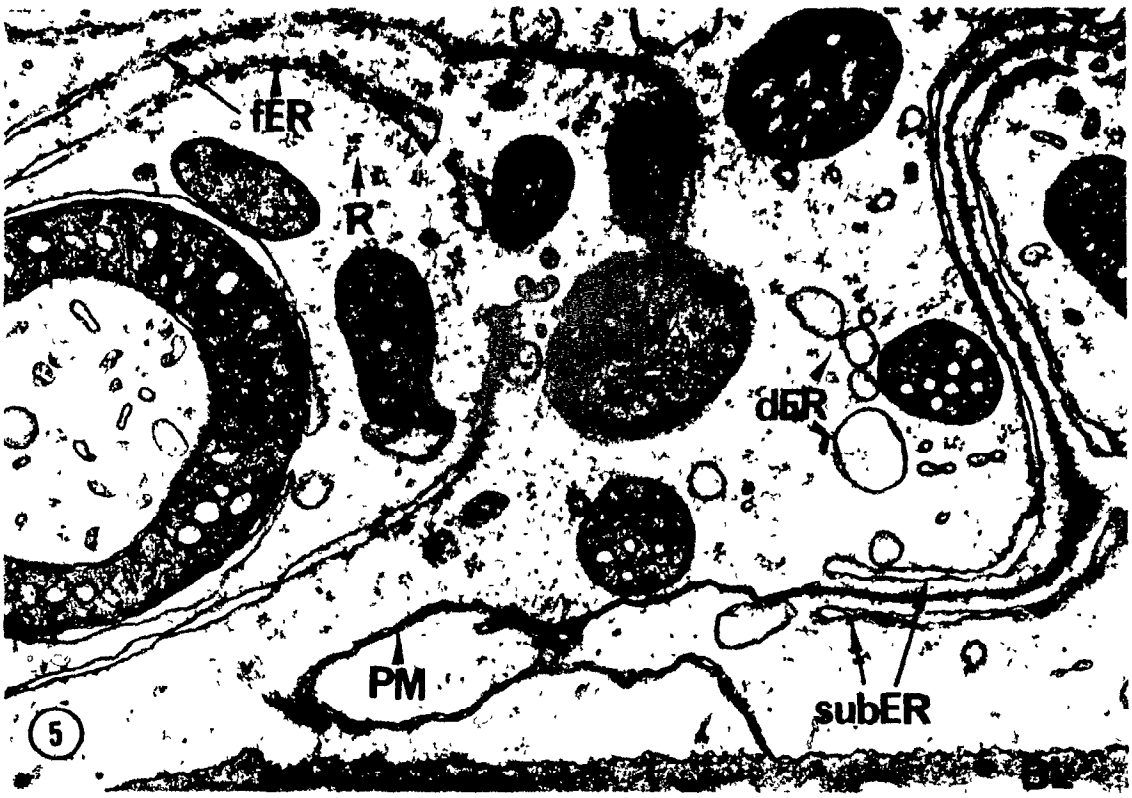
fER
R
dER
PM
subER
5

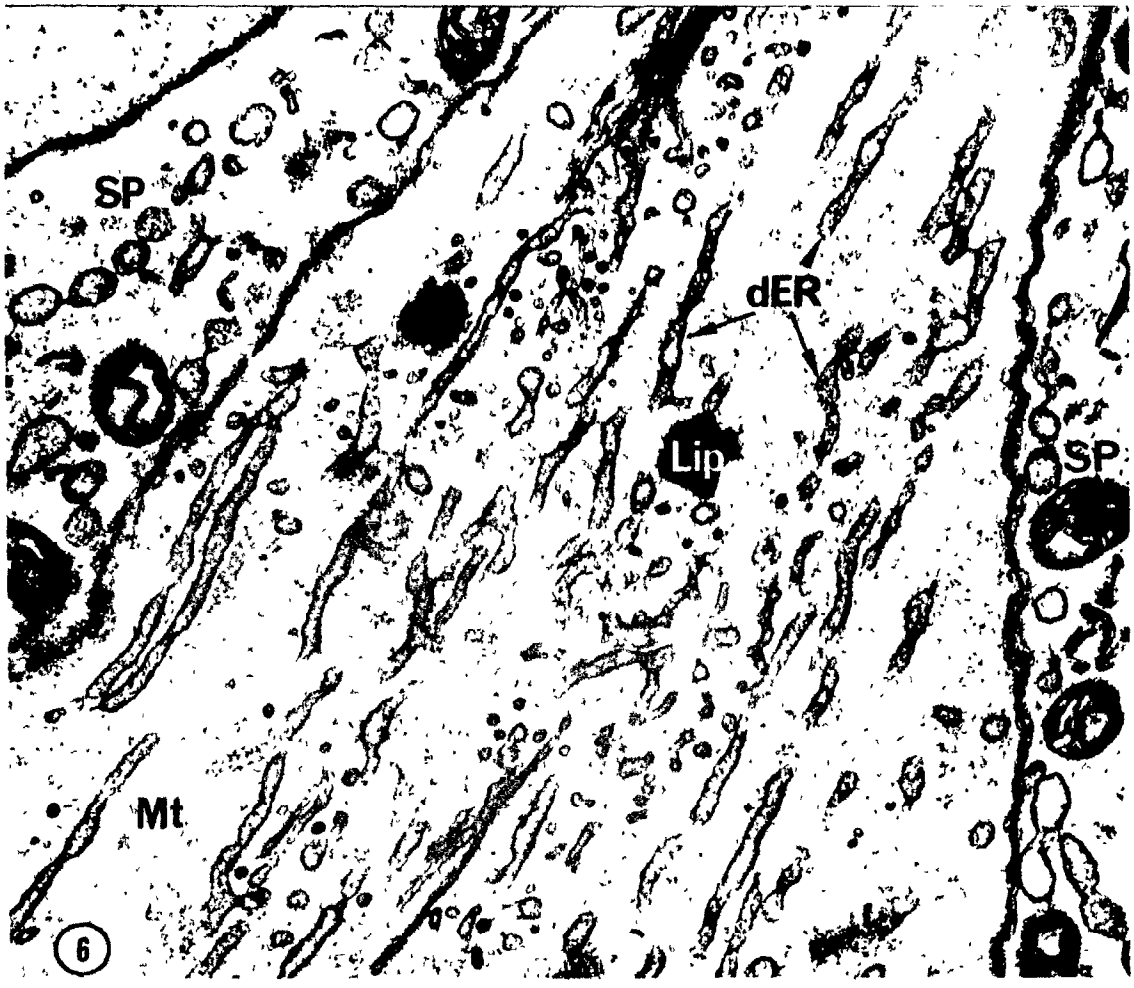
SP
dER
Lip
SP
Mt
6

FIGURE 7

The supranuclear portion of the Sertoli cell cytoplasm at stage XI of the cycle. (X 24,000)

Part of the nucleus (N) of the Sertoli cell is shown, as well as a portion of a primary spermatocyte (P).

The late spermatids (SP) are deeply inserted in the Sertoli cell cytoplasm with subsurface elements of ER (subER) seen parallel to their acrosomic system.

Numerous membrane-bound granules representing secondary lysosomes (L) are seen. One dense core granule (DC) or primary lysosome is also present. Finally, this photograph also shows a collection of tiny microvesicles (CM).


subER
dER
GM
L
DC
P
Gs
N
Lip
7

FIGURE 8

Basal region of a Sertoli cell at stage I of the cycle. (X 30,000)

The basal lamina (BL) can be easily identified. The photograph shows tubular elements of the Golgi apparatus (Gt), a lysosome (L) with an irregular outline and a membranous vacuole just to the left of it. Various profiles of mitochondria (M), flattened elements of the ER (fER) and distended elements of the ER (dER) are also seen.


dER
Gt
L
rER
O
BL

FIGURE 9

Junction between two adjacent Sertoli cells showing the plasma membranes (PM) of both cells and sub-surface elements of ER. (X 30,000)

The Sertoli cell above this junction includes a portion of the nucleus (N) and a large lipid droplet surrounded by flattened elements of ER (fER) of the rough variety. These elements are also seen associated with mitochondria (M). The second Sertoli cell, below the junction, shows a cross section of a tubulobulbar complex (TBC) that derives from the inter-Sertoli cell's junction.

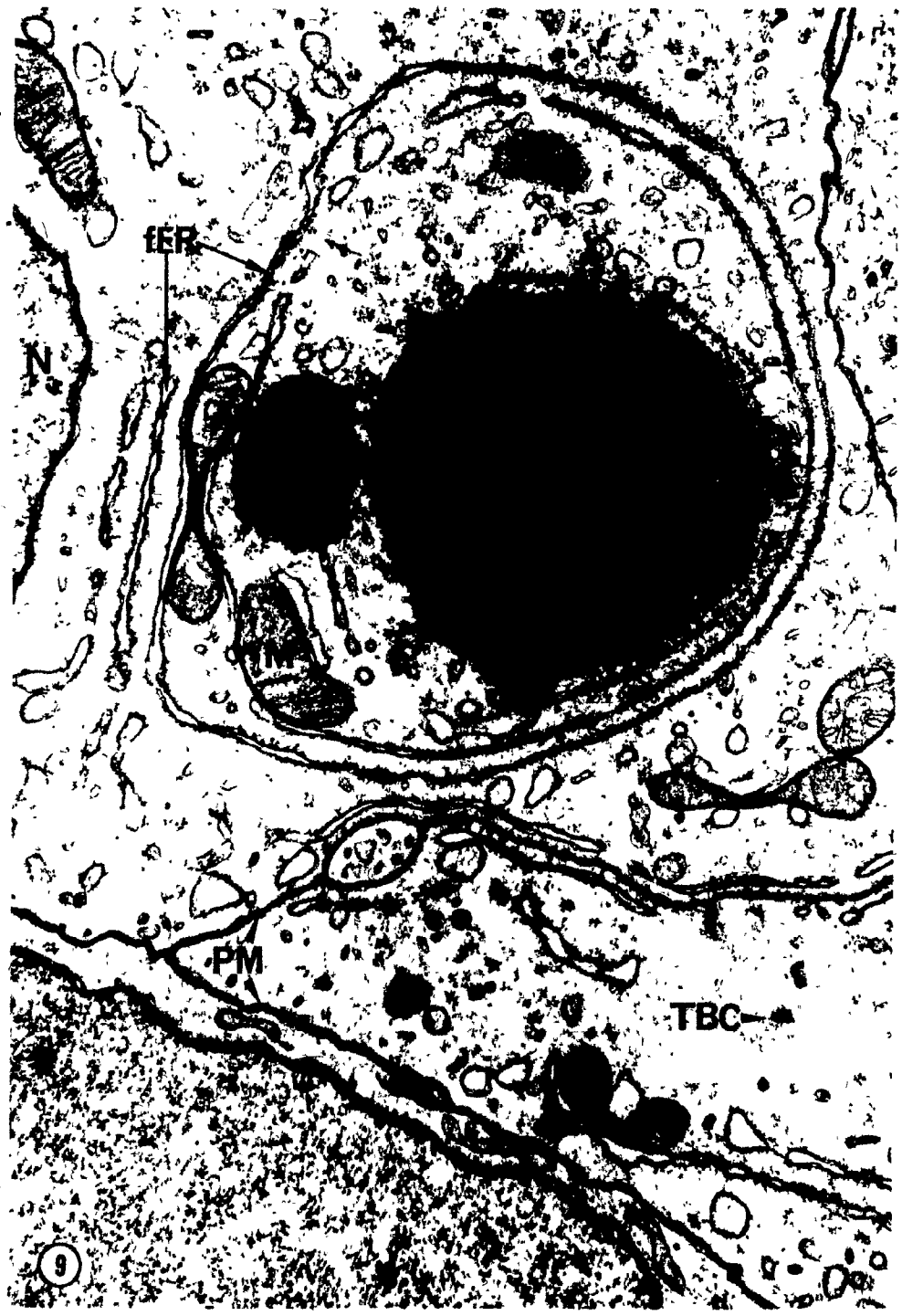
fER
N
M
PM
TBC
9

FIGURE 10

The relative volume of the three subcomponents of the endoplasmic reticulum in the Sertoli cell cytoplasm at the 14 stages of the cycle of the seminiferous epithelium.

The volume of the subsurface elements of the ER decreases significantly at stages VII, VIII and IX of the cycle. The volume of the flattened elements of the ER not associated with the plasma membrane increases markedly at stages VII and VIII of the cycle. The volume of the distended elements of the ER also varies throughout the cycle of the seminiferous epithelium with high values at stages X-XIV and I-III, intermediate values at stages IV-VII and low values at stages VIII and IX of the cycle.

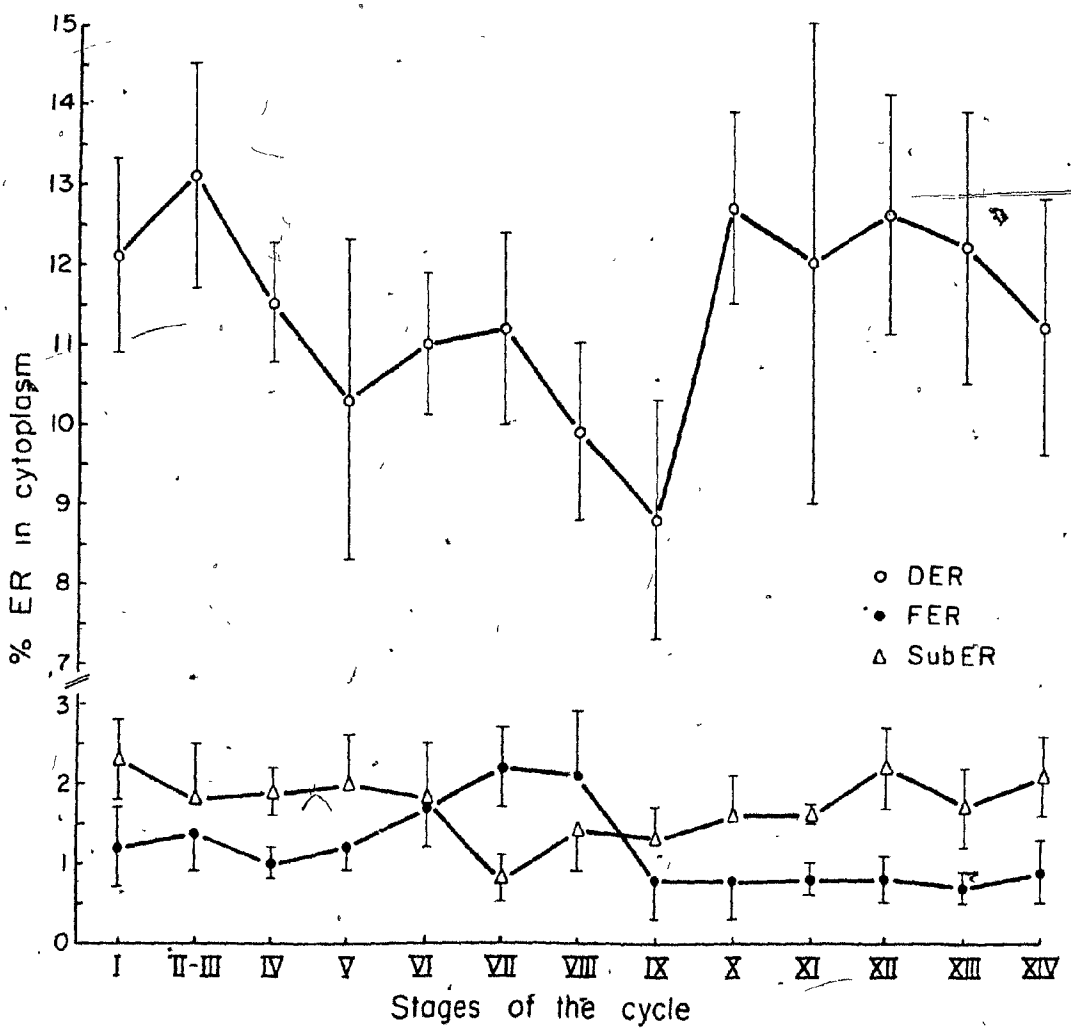
% ER in cytoplasm
15
14
13
12
11
10
9
8
7
3
2
1
0
o DER
• FER
Δ SubER
I
II-III
IV
V
VI
VII
VIII
IX
X
XI
XII
XIII
XIV
Stages of the cycle

(10)

FIGURE 11

The relative volume of both saccular and tubular components of the Golgi apparatus in the Sertoli cell cytoplasm at the 14 stages of the cycle of the seminiferous epithelium.

The volume of the saccular elements of the Golgi apparatus is fairly constant throughout the cycle with slightly lower values at stages XII and XIV. The volume of the tubular elements of the Golgi apparatus shows the pattern of a bimodal curve with two peaks, one at stages II-III and the other at stage X of the cycle. High values are recorded at stages I-V and X, intermediate values at stages VI-IX, XI and XIII and very low values at stages XII and XIV of the cycle.

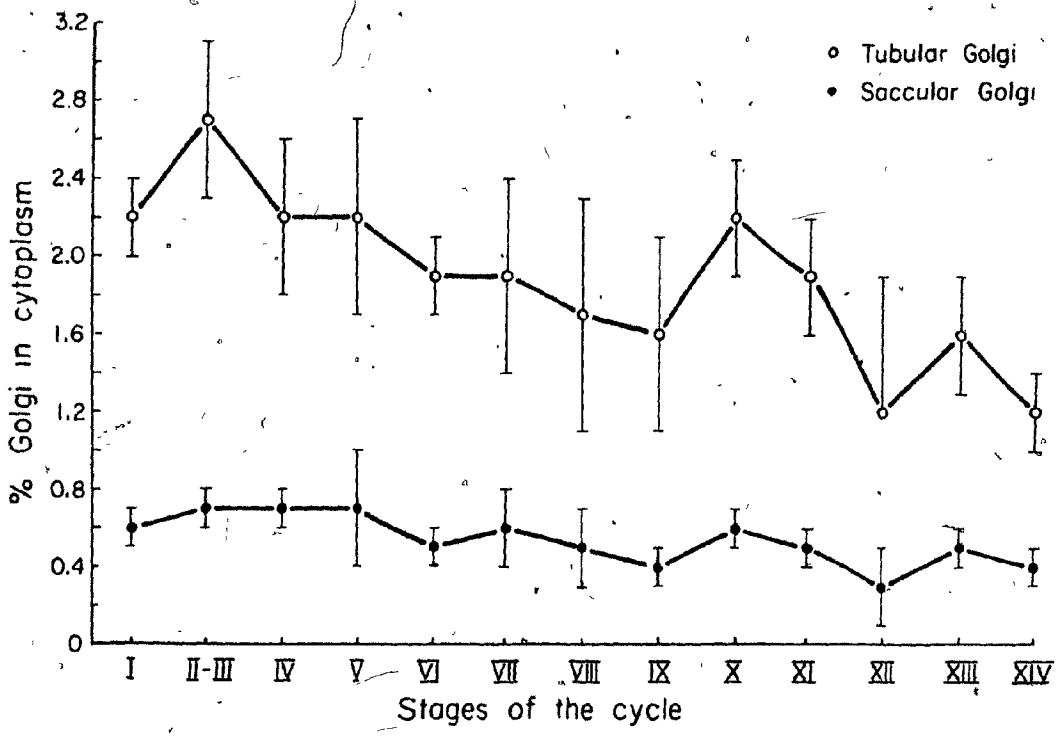
3.2
2.8
2.4
2.0
1.6
1.2
0.8
0.4
0
% Golgi in cytoplasm
Tubular Golgi
Saccular Golgi
I
II-III
IV
V
VI
VII
VIII
IX
X
XI
XII
XIII
XIV
Stages of the cycle

(11)

FIGURE 12

The relative volume of the primary and secondary lysosomes in the Sertoli cell cytoplasm at the 14 stages of the cycle of the seminiferous epithelium. The volume of the primary lysosomes makes up a small fraction of the overall volume of the lysosomal population, and remains constant throughout the cycle.

The volume of the secondary lysomes increases gradually from stages I to VI where it reaches a maximum at stages VI, VII and VIII and then decreases dramatically at stage IX and remains low from stages IX to XIII. It then increases at stages XIV and I and this pattern repeats itself at every cycle of the seminiferous epithelium.

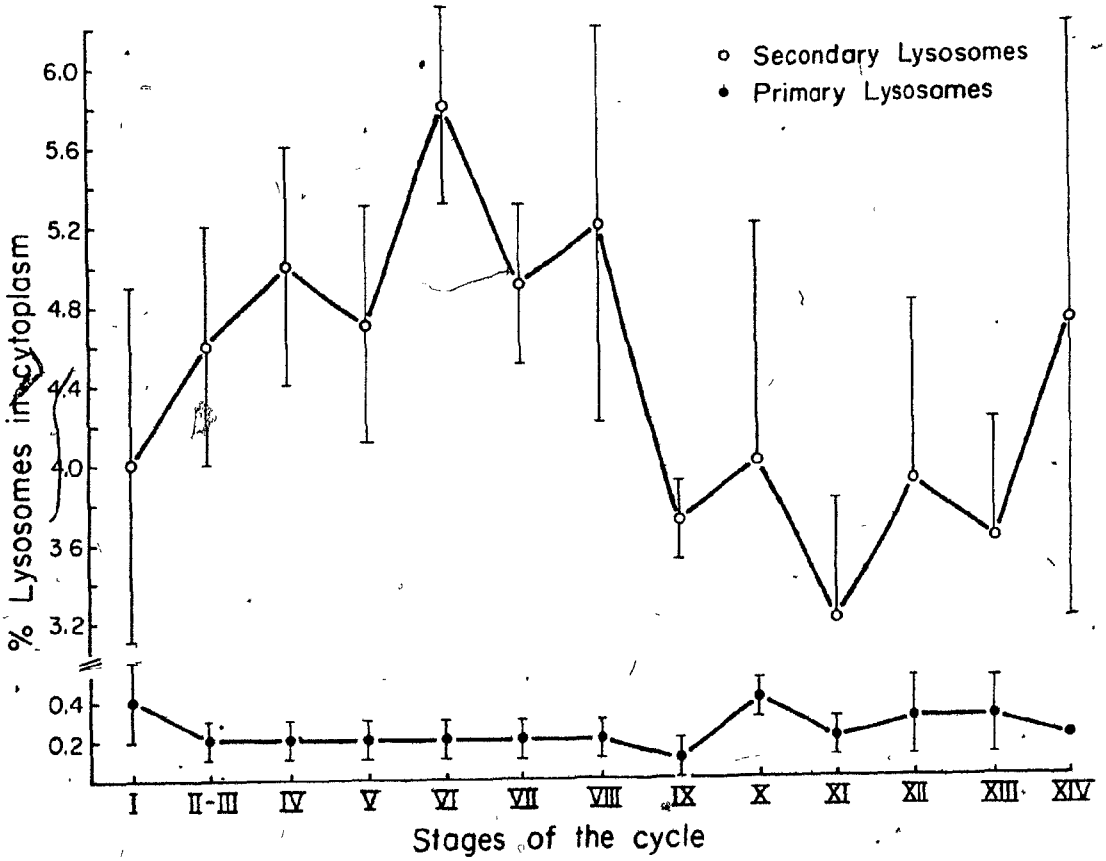
Secondary Lysosomes
Primary Lysosomes
% Lysosomes in cytoplasm
6.0
5.6
5.2
4.8
4.4
4.0
3.6
3.2
0.4
0.2
I
II-III
IV
V
VI
VII
VIII
IX
X
XI
XII
XIII
XIV
Stages of the cycle